Internship Report

Gaps, weeds or cane? Exploring PlanetScope multispectral imagery for classification during sugarcane emergence

Submitted by:
Nik Verweel
Registration Number: 1012884

Period of internship:
20/10/2025 - 27/02/2026

Supervisor:
Timon Weitkamp
RS Researcher
SmartCane

WUR Supervisor:
dr. HM Barholomeus

Date:
February 9, 2026

SMARTCANE

WAGENINGEN
UNIVERSITY & RESEARCH

Contents

List of Figures

List of Tables

1 Introduction

1.1 Professional context

SmartCane combines agricultural expertise with digital solutions to empower farmers, boost productivity, and transform smallholder sugarcane farming for social and economic impact. The company offers a range of remote-sensing-based tools to improve productivity, enhance sustainability, and contribute to food security. These solutions can be tailored at the farmer level, recognising their unique characteristics, or applied at a broader scale for creating overviews for wide outgrower networks. The tools SmartCane offers include yield prediction, irrigation planning, crop and market modelling, and behaviour tracking. Technically, the used models to achieve these services are wide-ranging, from data thresholding to spatial covariance calculations. Together with local SmartCane ambassadors in active countries such as eSwatini, Kenya, Uganda and Tanzania, client engagement and field validation drives active development of the available products and their quality, not just focussed on model quality, but also data delivery methods and their effectiveness. With strong connections to companies like Resilience and SmartFarming, SmartCane has a strong position in the market and aims to scale up production and expand its client base across Eastern Africa and Mexico. During the iterative improvement process of SmartCane's services, it has been noticed that certain clients have highlighted the need for early detection of gaps in sugarcane emergence. This would be valuable to properly monitor the initial growth stages of the sugarcane crop. Such a monitoring system should not only identify the presence of gaps but also their location, and ideally provide information on the potential for gap-filling (i.e., whether there is an identifiable problem in the field, such as soil moisture or nutrient deficiencies). Furthermore, in areas where vegetation growth is detected, it is valuable to distinguish between sugarcane and weeds, as the observation of growth alone does not guarantee that it originates from sugarcane, and weeds can also be problematic.

Such an early detection tool for gaps and weeds is currently provided on a limited basis to certain clients, exploratory in nature, with the functions still being tested and actively developed. Current methods to detect gaps are somewhat lacklustre. At the field level, the lower quantile of created chlorophyll index (CI) maps is taken, effectively classifying 25% of pixels within a field as a gap. Weed detection has been further developed, with a time-series analysis of the CI at pixel level. If the CI rises too quickly within a week, the pixel is noted as likely weed growth. This information is then generalised as a percentage of the field and fed back to the client. Currently both methods are applied using PlanetScope imagery, with the intention of further developing these methods to improve the quality of results and feedback, for which this exploratory research project was set up.

1.2 Scientific context

The clients' requests are not unfounded. Germination and tillering, sometimes referred to collectively as crop emergence, constitute a critical stage in the development of sugarcane, with the stage typically taking some three to four months. Low germination rates can result in substantial yield reductions and should therefore be monitored closely (Patel et al., 2014; Yadav et al., 2013). SmartCane reports that its clients typically assess germination approximately some three months after planting, checking for gaps in emergence at the plot or farm level. Where gaps are identified, additional sugarcane shoots may be planted to mitigate long-term yield losses. Similarly, early-stage weeds can have a negative effect on cane yield in the long term (Hussain et al., 2019; Rathika et al., 2023), and need to be removed from the field to prevent significant yield loss.

Currently the primary method of gap and weed identification under sugarcane farmers is through the visual inspection of the field, which requires extensive fieldwork by the farmer (Nakhone et al., 2025). While feasible for smallholder farmers living near their land, this process becomes increasingly time-consuming for those managing larger holdings or residing farther from their fields. As such, an automated system of gap and weed detection could benefit farmers through allowing optimised and specific field interventions. Preliminary research has found that this can be facilitated using spectral indices and spatio-temporal analysis, as existing research indicates that such methods are feasible later in the growth cycle (De Oliveira Maia et al., 2022; Mahadea-Nemdharry et al., 2025; L. F. Maldaner, Molin, Martello, et al., 2021; Rocha et al., 2022). In addition, numerous methods for general weed detection are available in the literature, with several approaches have been developed specifically for sugarcane. For example, differentiation between sugarcane and weeds has been shown to be possible utilising visible and Near Infrared spectroscopy through a Random Forest model (De Souza et al., 2019). Furthermore, approaches with machine vision have made spot-spraying of herbicides possible, showing that computer-vision aided detection of weeds is possible (McCarthy et al., 2009). While this suggests that the differentiation between cane, gaps and weeds might be feasible, the specific application of PlanetScope imagery during the emergence phase of the sugarcane growth cycle remains unexplored.

Exploring this application could then benefit farmers by potentially reliably identifying gaps or weeds during emergence, enabling targeted replanting and weed removal. Such an approach would allow rapid intervention and reduce potential yield losses, while simultaneously decreasing labour demands due to the automated nature of the process. As such, this research aims to address a knowledge gap in current literature by exploring methods to detect gaps and weeds during early sugarcane growth using PlanetScope imagery.

1.3 Internship objectives

This exploratory research aims to identify and develop methods to distinguish among emergent sugarcane, weeds, and gaps utilising PlanetScope imagery, as preliminary research suggests that there is theoretical applicability, though practical applications and examples are currently missing. To ensure relevance for the host organisation, the identified methods must be easily scalable and suitable for application to current processing pipelines, and as such a fully automated, script-based approach should be explored. Accordingly, the research objective of this internship is to explore and develop methods utilising PlanetScope imagery for the automated detection of gaps and weed growth during sugarcane emergence.

To address this objective, the following specific research questions (SRQs) have been formulated:

- **SRQ1**: What existing methods for sugarcane gap or weed detection using RGB imagery or band indices could be adapted for application to PlanetScope data?
- **SRQ2**: What method, if any, can be applied with PlanetScope data to accurately identify gaps during sugarcane emergence?
- **SRQ3**: What method, if any, can be applied with PlanetScope data to accurately differentiate between weed growth and sugarcane emergence?

1.4 Study area

While SmartCane is active across different countries and continents, the study area of this research has been defined as a number of sugarcane plots in the Morogoro region of Tanzania (Figure 1). In total, six fields covering 18.5 hectares were identified with an estimated field age of less than four months, meaning that the sugarcane in these fields is at most four months old (as of November 2025). Although this is slightly beyond the three-month emergence window, including fields up to four months ensures a broader range of data for method development. Each field has a unique name, and ages vary between approximately 2.5 and 3.8 months at the time of writing, which makes them well-suited candidates for exploring the detection of gaps and/or weeds, as they have recently emerged and canopy closure has not yet set in. Due to the absence of exact data from the farmers, the age of the fields is estimated based on field observations and expert opinion by SmartCane colleagues. Table 1 lists the different fields, their age, and their respective size.

Table 1: Overview of plots in study area

Client	Field	Age (months)	Size (ha)
Katembo	Field A	3.8	8.1
Moh	Mo1	3.5	0.6
Moh	Mo5	3.5	0.8
Shabani	Sha2	3.5	0.2
Mbigiri	Field A	2.8	4.5
Yusuph	Field A	2.8	4.3

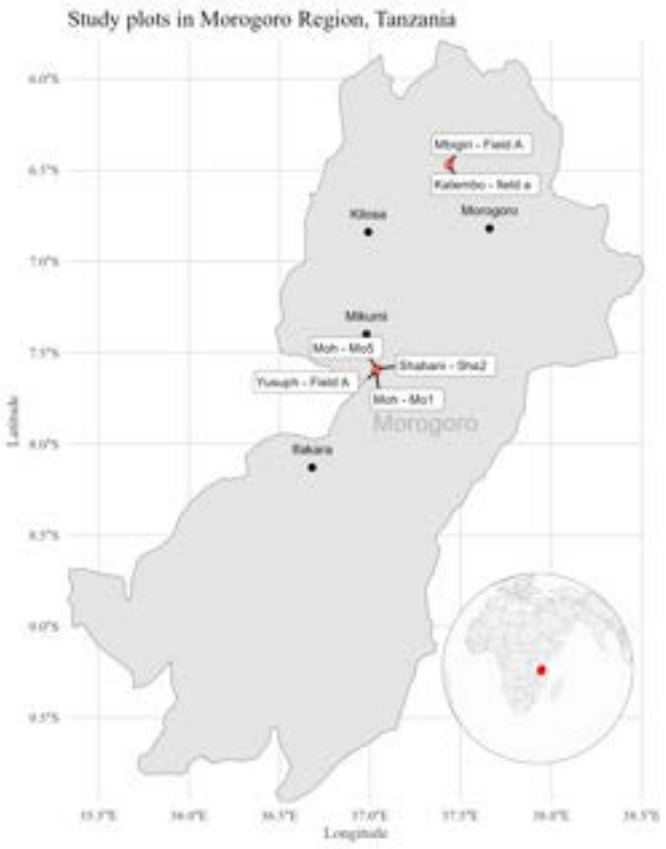

Figure 1: Location of study plots in Morogoro, Tanzania

2 Methods

2.1 Data

2.1.1 PlanetScope

Given the research aims and current workflows at SmartCane, the primary source of data for this project is PlanetScope satellite imagery. PlanetScope imagery is provided by Planet Labs, a commercial satellite company, and has higher spatial resolution than open-access satellite data sources such as Sentinel imagery. The imagery is collected by a constellation of approximately 180 'Dove' and 'SuperDove' satellites, enabling daily revisit times at nadir. PlanetScope imagery has a spatial resolution of 3.0–4.1 meters at nadir and comprises 8 spectral bands, as summarised in Table 2 (Planet Labs Inc., 2021).

Table 2: Spectral band information of PlanetScope imagery

Spectral Band	**Wavelength (nm)**
Coastal Blue	431 - 452
Blue	465 - 515
Green I	547 - 583
Green	547 - 583
Yellow	60 - 620
Red	650 - 680
Red Edge	697 - 713
Near Infra Red (NIR)	845 - 885

The imagery is provided as a Level 3A product, meaning that the data have been orthorectified with pixel values representing surface reflectance, ready for analysis. In addition to the spectral bands, the imagery includes a "Usable Data Mask" layer, which provides cloud cover classification and enables masking of cloudy pixels. In total for this study, PlanetScope imagery of the study area was retrieved for the periods of 7-30 November 2025 and 15-28 December 2025, totalling 22 images, to be used during different phases of the project as further explained in this Section.

2.1.2 Field data

The methods described in Section 2.2.5 saw need of field data for the purposes of training supervised classification models. During the inception phase of this research project, broad acquisition of this field data was planned with local partners, but this failed to materialise. Local geo-political circumstances in Tanzania hindered the data collection efforts, and in the end only five field observations were performed. These field observations were conducted between 22 October and 3 December 2025 by a colleague in the field, with the data collected using the Open Data Kit (ODK) platform. The data included information such as the GPS location (taken from a mobile phone, with an accuracy of at best ±4m and at worst ±10m; J. van der Most, personal communication, 24 November 2025), plant health, plant age, growth stage, soil conditions, weed presence, and a photo of the field conditions at the visited point.

2.2 Methodology

2.2.1 Literature review

To answer the first SRQ and identify existing methods for gaps and weed detection applicable to PlanetScope imagery, a literature review was conducted. During this literature review, the Preferred Reporting Items for Systematic reviews and Meta-Analyses (PRISMA) statement was largely followed (Page et al., 2021), graphically summarised in Figure 2, tracked through the PRISMA checklist and flow diagram. While one of the checklist items states that any scientific article performing a PRISMA review must feature "review" in the title, this was decided against due to the review being a specific research goal, rather than the main research goal. Similarly, the specifically outlined abstract guidelines were not followed.

For the review, the Scopus database was utilised, with the search conducted on October 28$^{\text{th}}$ 2025. The search query "(Sugarcane OR 'Sugar cane') AND (gap OR weed*) AND detection AND NOT 'deep learning'" was used, with a search filter for article abstracts, limited to articles and review papers between 2010 and 2025, in English. Both spellings of sugarcane were included as both are used in the literature. "Gap" and "weed*" were included to find articles that pertain to the research objectives. The asterisk in "weed*" allowed the inclusion of both the term "weed" and "weeds". The term "deep learning" was excluded as the vast amounts of labelled training data typically required for constructing such a model were not available. Considering the purpose of the review, inclusion criteria were developed to identify records that were theoretically applicable to the available PlanetScope data. Records not meeting the inclusion criteria were excluded. Articles were included based on (1) relevance to the research objectives, (2) suitability to the available data, and (3) description(s) of the method used. In practical terms, relevance to the research objectives means that the record includes some knowledge pertaining to the detection of sugarcane, gaps or weeds. Suitability to the available data refers to the constraints of satellite imagery with spatial resolution equal or worse than the PlanetScope imagery. For example, high-resolution Unmanned Aerial Vehicle (UAV) imagery is not comparable to the available imagery, and thus it is highly unlikely that methods relying on the high spatial resolution will function well when attempted with PlanetScope imagery. Finally, the record must either directly describe the method applied in enough detail to allow adaptation, or reference a source that does so. This ensures that SRQ2 and SRQ3 can be achieved using methods identified during the literature review.

Records identified with the initial search query were first screened for relevance by their title and abstract. During the screening, records that had no obvious relevance to this research were removed. Following this, the remaining records were sought for retrieval and assessed for their eligibility according to the outlined inclusion criteria. The number of records excluded, assessed, and included was tracked in the official PRISMA flowchart.

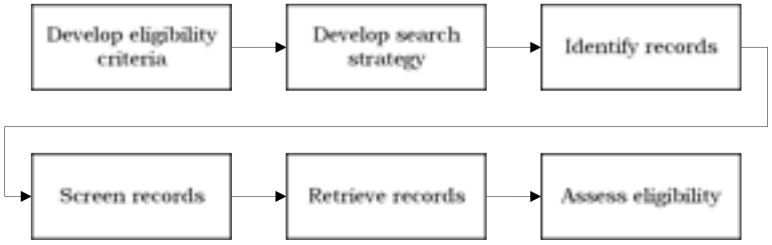

Figure 2: Graphical summary of the PRISMA approach to literature review

2.2.2 Data preprocessing

Prior to the application of any methods found through the literature review, the retrieved PlanetScope imagery was pre-processed. In many remote sensing applications, the presence of clouds and cloud shadows has been known to be disruptive to the approaches taken (Gawlikowski et al., 2022). Especially when applying methods to optical data, such as PlanetScope imagery, clouds can block the line of sight, and haze and cloud shadows can influence the spectral pattern (Pearce, 1985; Shastry et al., 2023). As such, the detection and filtering of clouds is important to reduce their effects where possible. This is one of the reasons that PlanetScope imagery is supplied with a specific cloud masking layer, providing a binary classification between cloudy pixels and non-cloudy pixels. However, this cloud masking layer is not always sufficient, as is evidenced by the number of articles which aim to develop an improved cloud-filtering algorithm for PlanetScope imagery (Frazier & Hemingway, 2021; Shendryk et al., 2019; J. Wang et al., 2021). As such, an alternative cloud-masking algorithm was explored as preprocessing step. While there are many alternative cloud masking models, OmniCloudMask (OCM), developed by N. Wright et al. (2025), is reportedly an appropriate model for PlanetScope imagery, with the sensor-agnostic deep-learning model boasting excellent accuracy. In addition to reportedly better accuracies, OCM classifies clouds into three classes: thick clouds, thin clouds and cloud shadows. In contrasts, the PlanetScope cloud mask layer only identifies thick clouds.

Given these excellent results, the OCM model was attempted as a means to ensure PlanetScope imagery being used for further application was of good quality. For a selection of available PlanetScope images from eSwatini, OCM was applied using the `omnicloudmask` Python package. Specifically, the function `predict_from_array` was applied using the red, green and near-infrared bands of the PlanetScope images. This method was applied at multiple spatial resolutions to assess the results. OmniCloudMask documentation suggests that the model works best at 10m. Given the spatial resolution of the images available, a resolution of 9m was selected instead as this allowed relatively easy downsampling and upsampling. In addition, the model was applied to the native resolution of the available imagery, resulting in two different OCM classifications.

Despite the reported accuracies, a comparison of PlanetScope's cloud mask classification and the two OCM classifications show that OCM generally over-classifies the presence of clouds to a level where images became unusable as the majority of data is masked out. An example of this is visualised in Figure 3, which shows the comparison between an unmasked, a PlanetScope-masked and OCM-masked image taken on 26 October 2025 near Phuzuoya, eSwatini. Given this over-classification of OCM, regardless of the reported accuracies, it was decided to apply only PlanetScope's own cloud masking band, given that OCM masking would render most images unusable. While this introduces some risk, particularly with regard to wispy clouds and cloud shadows, thick clouds are generally masked well, and more data remains to work with in the following steps.

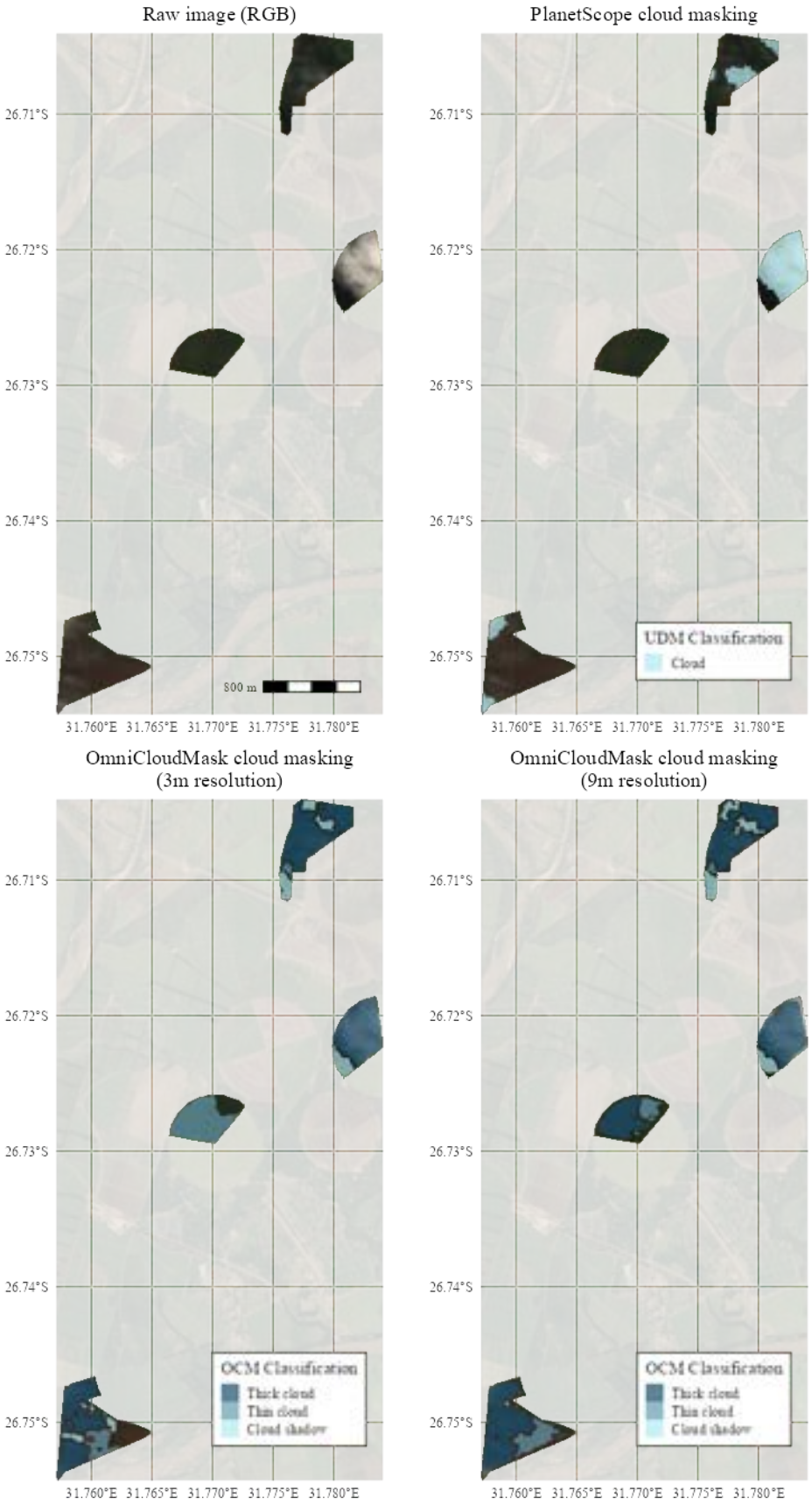

Figure 3: Comparison of different cloud-filtered PlanetScope images for plots in eSwatini

2.2.3 Feature engineering

Following the cloud masking of the individual images, feature engineering was performed based on the results of the literature review as presented in Section 3.1. Table 3 was used as a guide, and all spectral indices presented in it were calculated using the presented formulae through simple raster calculations. This resulted in a 14-band raster for each PlanetScope image, each band containing a raster of one of the calculated spectral indices.

In addition to the calculation of the spectral indices, the mean weekly difference for each index was also calculated. Based on the ISO-8601 week numbering, all 14-band rasters within a given week were mosaicked using `terra`'s `mosaic` function with the `mean` argument, chosen to potentially smooth out noise in the images if present. This resulted in average values (where multiple images overlapped) for the different indices per week. Following this, the weekly difference per spectral index was calculated using raster algebra by subtracting the previous week's mosaic from the current week's mosaic iteratively for each week. Where the two mosaics did not overlap, the difference values were set to `NA`.

Following these steps, the initial imagery available was combined into four mosaics covering weeks 46, 47, 51 and 52 of 2025, with each mosaic containing 28 bands: 14 bands with spectral indices, and 14 bands with their weekly change since last week. The feature engineering process as a whole is graphically summarised in Figure 4.

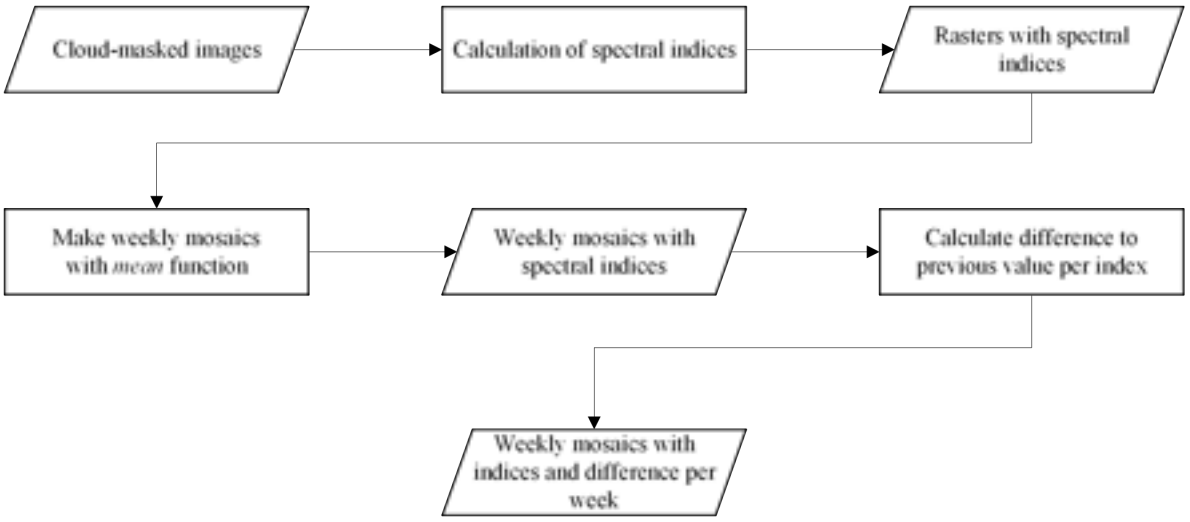

Figure 4: Graphical summary of the feature engineering processes

2.2.4 Supervised training data

Some of the methods identified during the literature review required training data for the training of supervised classifier models. Due to the difficulty obtaining field data, as explained in Section 2.1.2, the creation of training data required manual creation of training polygons based on the limited field observations, consideration of spectral index seasonality, and expert opinion. To facilitate this, historical values of all spectral indices were determined and plotted, allowing the identification of seasonal patterns in 11 of the 14 indices (Appendix I). By comparing pixel values, examining RGB imagery, and incorporating available field data, polygons were drawn in QGIS within the study area and assigned to cane, weed, or gap classes.

In total, twenty-eight polygons were created using this method based on the Week 48 (2025) mosaic image: twelve classified as cane (469 pixels), four as weeds (166 pixels), and twelve as gaps (370 pixels), shown in Figure 5. Distinguishing gaps from vegetation was relatively straightforward, whereas differentiating sugarcane from weeds required closer attention due to their spectral similarity.

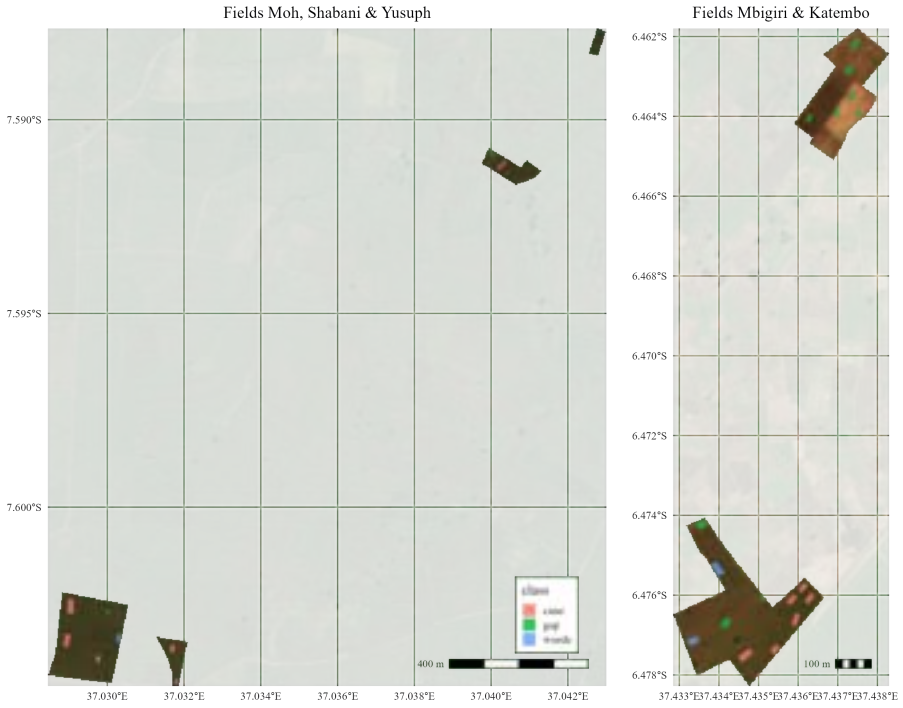

Figure 5: Overview of training polygons

2.2.5 Supervised classifiers

Following the feature engineering and training data preparation, various supervised classifiers were trained in `R` based on the results presented in Section 3.1. Given the results, five different models were created: a Random Forest, an Extreme Gradient Boosting, Linear and Radial Support Vector Machines, and a Linear Discriminant Analysis model. Conceptually, each classifier has its own strengths and weaknesses. Random Forest is a widely used machine learning model with many use cases, including the classification of sugarcane (Waters et al., 2024). It functions by constructing hundreds of decision trees and aggregating their votes, making it well-suited for classification tasks (Abdi, 2019). Extreme Gradient Boosting builds decision trees sequentially rather than simultaneously, enabling iterative model improvement. With more opportunity for tuning, Extreme Gradient Boosting can outperform Random Forest in certain settings (Khuc et al., 2025). Radial Support Vector Machine, while having high computation costs, allows for complex boundary shapes between classes, facilitating the distinction between classes with similar spectral signatures such as sugarcane and weeds (Melgani & Bruzzone, 2004; Shi & Yang, 2015). Linear Support Vector Machine and Linear Discriminant Analysis are generally easier to work with, as they require relatively little tuning and have lower computational costs. However, they rely on the underlying assumptions that the data is linear, but not co-linear (M. Chen et al., 2018; Pirotti et al., 2016). Given the similar spectral patterns for cane and weeds, co-linearity needed to be mitigated through the removal of colinear variables. Through the development and comparison of these models, well-performing models could be identified to work towards answering SRQ2 and SRQ3.

For all classifiers, model training data were created by loading the raster(s) and previously created training polygons and using `terra`'s `extract` function, extracting all pixel values within the polygons to a DataFrame. The extracted data were cleaned by removing `NA` values, as they interfere with some models like Random Forest. Following this, the extracted data were split into training and test sets to allow for outer spatial cross-validation. The split was performed spatially to reduce the effects of spatial autocorrelation, which can significantly bias performance estimates (Ploton et al., 2020). Practically, this involved identifying unique polygon IDs, and applying stratified splitting into 70% training and 30% testing sets per class, and subsetting the data accordingly. This split enabled the evaluation of model performance on unseen spatial subsets through cross-validation. Subsequent steps differed by model type, as described in the following paragraphs.

Random Forest Classifier
Prior to training the Random Forest model, the training data were class-balanced to reduce the bias towards classes with higher frequency, particularly the sugarcane class. Through `caret`'s `downSample` function, the amount of data per class was balanced among the three classes. Following this, the Random Forest model was trained using the `ranger` package. The number of trees was set to 500, and the number of variables to possibly split at each node (`mtry`) was set to the default value (the square root of the number of variables). The variable importance mode was set to `permutation` to avoid bias, as `permutation` is recommended for data with high cardinality, as is the case with the calculated indices and rate of change rasters (Rihan et al., 2025). After training, the model was evaluated on the spatial hold-out set. Further model assessment is outlined in Section 2.2.7.

Extreme Gradient Boosting
Similarly to the Random Forest classifier, class weights had to be balanced for the Extreme Gradient Boosting model. In contrast to the Random Forest model, class distribution was balanced by normalising the frequency of class pixels relative to the total number of rows. This yielded a class weight vector used during training, necessary because `caret` does not support downsampling for Extreme Gradient Boosting. In addition to class balancing, a 5-fold inner spatial cross-validation was set up to allow for automated hyperparameter tuning. The model was trained through `caret` with a tune length of 50 (i.e., 50 random iterations of the hyperparameters, assessed against the inner folds) using `kappa` as the metric. `Kappa` was the preferred reporting metric as it provides clearer insight into model performance without the relative bias towards larger classes (Mellor et al., 2015). After training, this model was also tested on the spatial hold-out set.

Linear Support Vector Machine
The class weights and 5-fold inner spatial cross-validation were set up identically to those of the Extreme Gradient Boosting model. In addition to this, the data were centred and scaled within `caret`'s `train` function, a step required for Linear Support Vector Machines as the model is distance-based; unscaled variables with large ranges can influence the geometry and regularisation, potentially affecting model results. Following this, automated hyperparameter tuning was applied with a tune length of 10, again using `kappa` as the metric. Following model training, the model was tested on the spatial hold-out set.

Radial Support Vector Machine
The control parameters for the Radial Support Vector Machine followed those of the Linear Support Vector Machine, with class weights, 5-fold inner spatial cross-validation, centring and scaling set up identically. The model was trained with automated hyperparameter tuning, also with a tuning length of 10, using the `kappa` metric. Once again, the trained model was tested on the spatial hold-out set.

Linear Discriminant Analysis
Finally, the Linear Discriminant Analysis model was trained. Prior to training, variables with high collinearity were identified and removed, as the model is highly sensitive to collinear variables. Then, similar to previous models, control parameters were configured using down-sampling to balance class weights and a 5-fold inner spatial cross-validation. The model was trained without hyperparameter tuning, as `caret` does not support it for Linear Discriminant Analysis. Following training, the model was tested on the spatial hold-out set.

Following classifier training, all models were applied to classify the Week 47 mosaic image. Three outputs were generated: individual classification maps for each model, a majority classification layer for the non-linear models, and a layer indicating the number of non-linear models in agreement. Classification was performed using `terra`'s `predict` function with `na.rm = TRUE`, necessary because the Random Forest model cannot handle missing values. The majority classification was computed using `terra`'s `modal` function, which determines the mode across different bands within a raster. For ties in the mode calculation, the `ties` parameter was set to `"first"`. The different outputs - individual classifications, majority classification, and model agreement count - were combined as separate bands into a single raster, allowing inspection of each layer independently using software such as QGIS.

2.2.6 Unsupervised classifiers

Due to difficulties obtaining robust field training data (Section 2.1.2) and the supervised classification results (Section 3.2), unsupervised classification was also performed, despite not being concrete finding during the literature review. Three different unsupervised classifiers were trained on the North-Eastern portion of the Week 48 mosaic, covering the Mbigiri and Katembo fields. This area was selected because it contained all classes and prevented training errors from the high volume of `NA` values that occurred when using the full mosaic.

K-means clustering
The first classifier trained was a k-means algorithm with three classes. K-means is one of the most straightforward and widely used unsupervised classifiers for solving clustering problems (Lloyd, 1982; Rashmi et al., 2016). Training was implemented in R using the `unsuperClass` function from the `e1071` package. The number of classes (`nClasses`) was set to 3 to direct the model to identify three distinct classes. A sample of 3000 pixels was used (`nSamples`), with 25 random starts and a maximum of 200 iterations.

ISODATA
Following the k-means clustering classifier, the Iterative Self-Organising Data Analysis Technique (ISODATA) method was attempted. Whereas k-means requires the user to specify the number of classes a priori, ISODATA is self-organising, starting with an initial number of clusters and iteratively splitting or merging them (Karthik & Shivakumar, 2021). No consensus exists regarding which method is superior, as ISODATA has outperformed k-means in some cases (Priyadarshini et al., 2018), and vice versa (Saad & Al-Zubaidi, 2025). Despite this, ISODATA was implemented using the `Rsagacmd` package (Pawley, 2024) in R, which enables

operations from the SAGA GIS toolkit (Conrad et al., 2015). Before clustering, the data were reprojected to the UTM Zone 36S coordinate system to ensure square pixels, required for SAGA GIS ISODATA clustering. Using the `isodata_clustering_for_grids` function, clustering was performed with the following parameters: data normalisation, 25 iterations, three initial clusters, ten maximum clusters, and a minimum sample size of 30 pixels per cluster.

Fuzzy c-means clustering
While k-means clustering assigns each pixel to a single discrete class, fuzzy c-means clustering allows pixels to have varying membership probabilities across classes (Demirhan, 2024; Dunn, 1973). This provides additional insights for edge pixels at class boundaries and areas of spectral mixing where class spectra overlap (Heil et al., 2018). As with k-means, 3000 pixels were randomly sampled from the image for model training. The `cmeans` function from the `e1071` package was utilised with three centres (representing the three classes), a maximum of 100 iterations, and the fuzzification parameter (m) set to the default value of two.

Following the training of the unsupervised models, all models were used to classify the Week 47 mosaic image. Individual classification maps were created for each model, with four classification outputs for the fuzzy c-means model. The k-means method, given its discrete nature, returned a classified raster when using `terra`'s `predict` function. Similarly, the clustering with the ISODATA method returned a discretely classified raster. However, the fuzzy c-means classification provided both hard and fuzzy classification outputs. For the hard classification (discrete interpretation of class membership probabilities), the squared Euclidean distance between every pixel and each cluster centre was calculated. The Euclidean distances per band were summed, resulting in three raster bands (one for each class) containing distance values to each cluster centre. Each pixel was assigned to the class with the minimum distance, effectively assigning it to its nearest cluster centre. For the fuzzy classification, the degree of membership per class was determined through the fuzzy membership matrix. Based on the Euclidean distances, D_{ij} and D_{ik}, calculated as during hard classification, the membership probabilities (between 0 and 1) per pixel, μ_{ij}, were determined using the fuzzifier, m, with the following equation:

$$\mu_{ij} = \frac{1}{\sum_{k=1}^{N} \left(\frac{D_{ij}}{D_{ik}}\right)^{\frac{2}{m-1}}}$$

The degrees of membership per class were saved as individual raster bands. The maximum membership value across the three bands was then compared against a user-defined threshold of 0.75 (representing 75% confidence). Pixels without a membership probability of 0.75 or higher in any class were assigned a value of -99 to represent unclassifiable pixels. Similarly to the supervised classification, classification results from the different models were stacked as bands into a single raster, enabling inspection of independent layers in software such as QGIS. In contrast to the supervised classification, no consensus map was created. Due to the unsupervised nature of the classification, class numbers are not consistent across methods; a class interpreted as gap may be labelled class one in one method and class three in another, rendering a consensus map impractical. In addition to this, cluster labels had to be assigned to relate the cluster numbers to the target classes (cane, weed, and gap). This was achieved by comparing the classified imagery with the supervised training data described in Section 2.2.4.

2.2.7 Model testing and validation

As described in Section 2.2.5, the supervised classifiers were trained using a 70/30 spatial train-test split. The 30% hold-out set was used for initial evaluation of model performance through confusion matrices and accuracy metrics including the Kappa score, class-wise F1 scores, and

balanced accuracy. The unsupervised classifiers, lacking labelled training data, could not be quantitatively assessed using these metrics.

In addition to the supervised classifiers' test metrics, both supervised and unsupervised classifiers were validated. Initial plans included validation against field data, but due to the constraints explained in Section 2.1.2, field observation retrieval was severely limited. Instead, an expert-based reference data collection framework was utilised, following the Land Cover Protocol by NASA's Land Product Validation subgroup (Tyukavina et al., 2025). The protocol offers multiple approaches; in this case, the *consensus interpretation approach* was used, which is more readily achievable with limited expert availability. The alternative *majority interpretation approach* relies on assigning the majority class from expert labels but may result in ties when fewer experts are involved, as is the case in this research project.

According to the consensus interpretation framework, two experts independently labelled imagery with the classes cane, weed, and gap, additionally assigning a confidence level (high, moderate, or low). Labels were drawn in a QGIS project prepared for this purpose. Two sets of labels were created for weeks 51 and 52 of 2025, based on RGB imagery from the relevant week and the derived feature layers (spectral indices, weekly mosaics, and weekly differences) described in Section 2.2.3. Experts were tasked with drawing polygons for different classes and confidence levels based on RGB imagery and the available spectral information. Rather than imposing rigid constraints, experts were requested to provide polygons in a range of sizes across all classes.

The labelling experts were T. Weitkamp, a Remote Sensing researcher at SmartCane who holds an MSc in International Land and Water Management, an MSc in Geo-information Science, and a PhD in Remote Sensing specialising in land cover classification, and J. van der Most, who holds an MSc in International Land and Water Management and has worked extensively with interpreting satellite imagery at SmartCane. After individual labelling, the experts' classifications were compared. Areas with conflicting classifications were discussed in a consensus meeting. Considering the experts' confidence levels and experience, consensus was reached for all disputed areas, yielding a final reference classification.

To enable quantitative validation, the labelled polygons were rasterised to match the grid and resolution of the classification rasters with `terra`'s `rasterise` function. Models were then validated against this expert reference classification through confusion matrices and accuracy metrics such as precision, recall, F1 and Matthew's Correlation Coefficient (Chicco & Jurman, 2020), allowing a definitive answer to the outlined research questions.

2.3 Materials

Due to the digital nature of this research, physical materials were not required. For digital processing, an ASUS Vivobook Pro X16, with an 11^{th} generation Intel Core i7-11370H (3.3GHz) processor, 16GB RAM, and NVIDIA GeForce RTX 3050 Laptop GPU was used. Python scripts, Jupyter Notebook scripts, and R scripts were developed and utilised in Microsoft's Visual Studio Code IDE. R version 4.5.1 was used throughout this research (R Core Team, 2025). Important packages used included `terra` (Hijmans, 2025), `sf` (Pebesma, 2018), `xgboost` (T. Chen et al., 2025), `caret` (Kuhn & Max, 2008), `e1071` (Meyer et al., 2024), and `ranger` (M. N. Wright & Ziegler, 2017). Python version 3.11.14 was used throughout this research. Important packages used included `OmniCloudMask` (N. Wright et al., 2025). QGIS Desktop 3.44.2 was used during the creation of training data, validation data, and for inspection of rasters in between processing steps.

3 Results

3.1 Literature review

The initial Scopus search to identify potential methods as part of SRQ1 identified 42 records. No duplicates were identified, and subsequently all 42 records were screened for relevance. Following the screening, 27 records were excluded. Of these 27 records, the majority discussed the effects of diseases, pests, herbicides or viruses, without a geo-spatial component, making them unrelated to the research aims of this project (Achon et al., 2016; De Araújo et al., 2025; De Assis et al., 2013; Gell et al., 2014; Jeyaraman et al., 2025; Kong et al., 2025; Li et al., 2024; Meng et al., 2019; Mgode et al., 2019; Mielke et al., 2023; G. Rao et al., 2011; G. P. Rao, 2021; Ratchawang et al., 2022; Williams et al., 2025; Wilson et al., 2023; Yahaya et al., 2018; Ying et al., 2023; Zhou et al., 2016). Furthermore, a significant number of records still made use of deep learning methods, in particular the You Only Look Once (YOLO) model, despite attempts to filter these out (Ajayi et al., 2024; Deng et al., 2025; Moazzam et al., 2021; Paleti et al., 2023; Rubini & Kavitha, 2024; Sujithra & Ukrit, 2022). Finally, several records discussed miscellaneous topics, such as water quality and human working conditions (Cappelini et al., 2012; d'Errico et al., 2025; Ferreira et al., 2011).

Relatively few of the initially identified records came from the African continent, with only one record from Nigeria, one from Tanzania, and one from Namibia. Instead, the majority of the research was focussed on Brazil (11 records), China (7 records), India (7 records), and the United States (6 records).

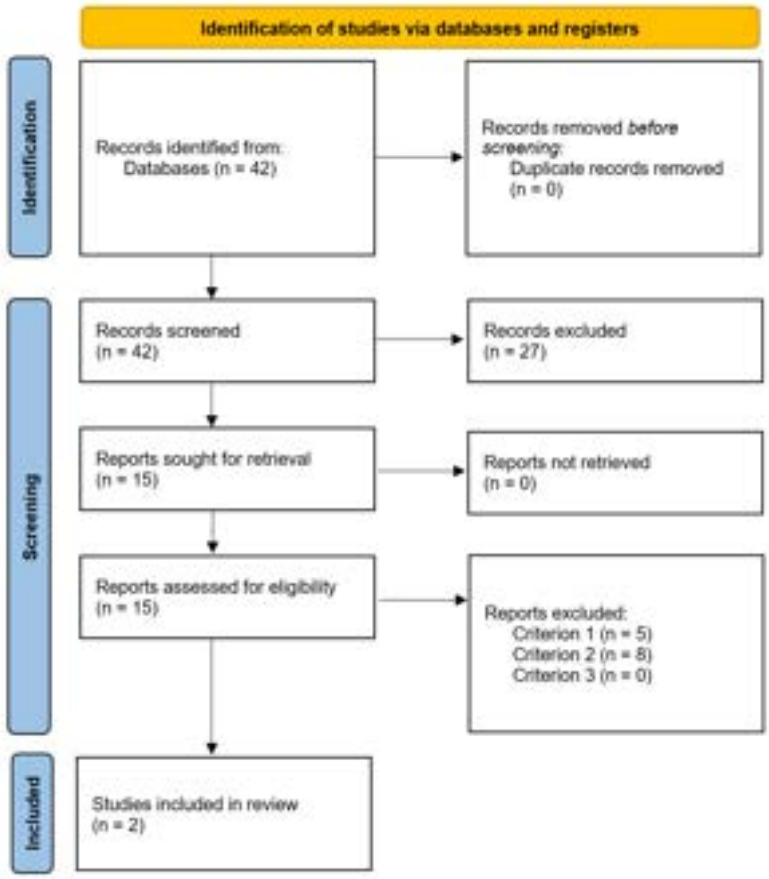

Figure 6: Overview of results after PRISMA literature review

Following the screening, 15 records were sought for retrieval and all were successfully retrieved. These reports were assessed for eligibility according to the outlined inclusion criteria. Criterion 1 led to the exclusion of 5 records. While the initial record screening did not reveal a fundamental mismatch with the research objectives through the assessment of the article abstract, further assessment of the whole article showed that these reports did not address the relevant objectives in sufficient detail (Bhatt et al., 2024; Johansen et al., 2017; Msomba et al., 2024; Pereira et al., 2020; H. Xu et al., 2025). A further 8 records were excluded according to criterion 2, with the majority excluded due to the use of UAV data, which does not match the spatial resolution of the available data (Di Girolamo-Neto et al., 2019; L. Maldaner et al., 2025; Panduangnat et al., 2024; Tanut & Riyamongkol, 2020; Thamoonlest et al., 2025). Furthermore, some reports were focussed on multispectral data obtained by robots in the field, which also led to a mismatch in the spatial resolution with the available data (Johnson et al., 2023; L. F. Maldaner, Molin, Canata, & Martello, 2021; Sujaritha et al., 2017). Criterion 3 did not lead to further exclusions. Figure 6 provides an overview of the identification process, and how many records were excluded at each step.

After assessment, two records remained to be included in this study, with both articles taking the approach of supervised classification development based on spectral indices. The review paper by Waters et al. (2024) focuses on satellite-based spectroscopy and machine learning methods for monitoring sugarcane health. While the review primarily identifies articles on pests and diseases, it covers different vegetation indices in detail. In total, 35 vegetation indices are listed, which could be used for feature creation to further refine threshold approaches to identifying gaps or weeds. A considerable number of the presented indices cannot be calculated using PlanetScope imagery, as they require specific wavelengths of light that are not available. Despite these limitations, several promising indices remain that can be utilised. Notable indices that are applicable to PlanetScope data are summarised in Table 3.

The paper further describes different machine learning methods applicable to health monitoring, generally highlighting the best results when applying Random Forest, Support Vector Machine, Extreme Gradient Boosting, Linear Discriminant Analysis or Radial Support Vector Machine models. These approaches, in combination with the outlined spectral indices, could allow the training of models to distinguish between gaps, cane and weeds through a comparison of index values.

Similarly, the second included record utilised a random forest model for a generalised classification model to identify sugarcane from Landsat-7 and Landsat-8 imagery (Luciano et al., 2018). Based on the imagery, and in particular the red, Near Infrared (NIR) and Short Wave Infrared (SWIR) bands in combination with multiple spectral indices, a random forest model with 500 trees and 13 predictor variables on monthly composite images (defined as the monthly median of high-quality images) was developed. The indices used include some already reviewed by Waters et al. (2024), including the Normalised Difference Vegetation Index (NDVI), Enhanced Vegetation Index (EVI), and the precursor of the Modified Soil Adjusted Vegetation Index (MSAVI). In addition to this, several water or moisture indices are mentioned, but these rely on the SWIR bands which are not available on PlanetScope imagery. The only additional index proposed by Luciano et al. (2018) which is applicable to PlanetScope imagery, is the Normalised Difference Water Index (NDWI), which is added to Table 3.

In addition to the reviewed literature, based on knowledge and experience at SmartCane, the Chlorophyll Index - Green (CI-G) and the Chlorophyll Index - Red Edge (CI-RE) are considered valuable information sources, as they are currently used in thresholding practices. Therefore, these indices have been added to Table 3 to be also be used as part of the model training.

Table 3: List of vegetation indices applied to PlanetScope imagery, adapted from Waters et al. (2024) and Luciano et al. (2018)

Author(s)	**Vegetation Index**	**Formula**
Rouse et al. (1974)	Normalised Difference Vegetation Index (NDVI)	$\frac{NIR-RED}{NIR+RED}$
Kaufman and Tanre (1992)	Atmospherically Resistant Vegetation Index (ARVI)	$\frac{NIR-(RED-BLUE)}{NIR+(RED-BLUE)}$
Tucker (1979)	Normalised Green Red Difference Index (NGRD)	$\frac{GREEN-RED}{GREEN+RED}$
A. A. Gitelson et al. (2002)	Visible Atmospherically Resistant Index (VARI)	$\frac{GREEN-RED}{GREEN+RED+BLUE}$
A. A. Gitelson et al. (1996)	Green Normalised Difference Vegetation Index (GNDVI)	$\frac{NIR-GREEN}{NIR+GREEN}$
A. Gitelson and Merzlyak (1994)	Normalised Difference Red-edge Index (NDRE)	$\frac{NIR-RedEdge}{NIR+RedEdge}$
Huete et al. (2002)	Enhanced Vegetation Index (EVI)	$2.5 \cdot (\frac{NIR-RED}{NIR+6 \cdot RED-7.5 \cdot BLUE+1})$
Vincini and Frazzi (2010)	Chlorophyll Vegetation Index (CVI)	$\frac{NIR \cdot RED}{GREEN^2}$
Zarcotejada et al. (2005)	Blue Green Pigment Index (BGI)	$\frac{BLUE}{GREEN}$
Louhaichi et al. (2001)	Green Leaf Index (GLI)	$\frac{(GREEN-RED)+(GREEN-BLUE)}{2 \cdot GREEN+RED+BLUE}$
Qi et al. (1994)	Modified Soil Adjusted Vegetation Index (MSAVI)	$\frac{2NIR+1-\sqrt{(2NIR+1)^2-8(NIR-RED)}}{2}$
McFeeters (1996)	Normalised Difference Water Index (NDWI)	$\frac{GREEN-NIR}{GREEN+NIR}$
A. A. Gitelson et al. (2003)	Chlorophyll Index - Green (CI-G)	$\frac{NIR}{GREEN} - 1$
A. A. Gitelson et al. (2003)	Chlorophyll Index - Red Edge (CI-RE)	$\frac{NIR}{RedEdge} - 1$

The results from the literature review highlight a vast range of spectral indices and modelling methods available that might be used to differentiate between sugarcane, weeds and gaps. Beyond the various indices for feature creation and modelling approaches, the temporal aspect merits consideration. While not explicitly mentioned in the assessed articles, current practices at the internship placement suggest that considering the rate of change in certain indices as a valuable feature for the classification effort could be beneficial.

3.2 Supervised classifier performance

3.2.1 Testing performance

After training the supervised models, they were tested against a spatial hold-out set, which was set aside during the training process. Based on the spatial hold-out set, the accuracy metrics presented in Table 4 were determined. Notably, Random Forest (RF), Extreme Gradient Boosting (XGB), and Linear Support Vector Machine (LSVM) all achieved similar metrics for the cane, gap, and weed classes. While performance was strong for cane and gaps with F1 scores approaching 1.00, weed classification was poor, with all weed pixels misclassified as cane. This occurred despite class-balancing during model training, likely due to the limited number of weed pixels in the spatial hold-out set (35, compared to 120 cane pixels and 145 gap pixels). Radial Support Vector Machine (RSVM) exhibited similar poor performance for the weed class but achieved better results for cane and worse results for gaps.

Somewhat surprisingly, Linear Discriminant Analysis (LDA) demonstrated the most promising results with the highest Kappa score and strong performance for both cane and gap classes. While weed classification remained challenging, LDA performed considerably better than the other models for this class.

Table 4: Testing performance by class, and model kappa score for supervised models.

	Cane				**Gaps**				**Weeds**				**Global**
Model	P	R	F1	BA	P	R	F1	BA	P	R	F1	BA	**Kappa**
RF	0.77	1.00	0.87	0.90	1.00	0.98	0.99	0.99	0.00	0.00	0.00	0.49	0.78
XGB	0.77	1.00	0.87	0.90	1.00	1.00	1.00	1.00	0.00	0.00	0.00	0.50	0.79
LSVM	0.77	1.00	0.87	0.90	1.00	0.91	0.95	0.95	0.00	0.00	0.00	0.48	0.72
RSVM	0.96	0.98	0.97	0.97	0.80	0.91	0.85	0.85	0.00	0.00	0.00	0.00	0.71
LDA	0.89	1.00	0.94	0.96	1.00	0.89	0.94	0.94	0.56	0.57	0.56	0.75	0.83

P = Precision, R = Recall, BA = Balanced Accuracy

In addition to the accuracy metrics, model testing provided insights into the relative importance of different features. Both the MSAVI and NDVI indices demonstrated high importance across models, as determined with `caret`'s `varImp` function. For the RF and XGB classifiers, MSAVI was the most important feature, with NDVI also ranking in the top three. For LSVM and RSVM, the top three most important features were identical: NDVI, ARVI, and NGRD. Notably, weekly difference features rarely appeared among the top ten most important features for these four classifiers. In contrast, the LDA model showed different patterns, with six of the ten most important features being weekly difference calculations. For LDA, NDRE, CVI, and BGR indices were the top three most important features. Complete feature importance data are summarised in Appendix II.

3.2.2 Validation performance

Comparison of the expert validation dataset with model classifications for weeks 51 and 52 provides a robust estimate of overall model performance. For each model, individual class performance metrics and overall accuracy are summarised in Table 5. The expert consensus classifications for weeks 51 and 52 are presented in Appendix III, and the supervised model consensus classifications for the same period in Appendix IV.

Table 5: Validation performance by class, and model accuracy for supervised models.

	Cane				Gaps				Weeds				Global
Model	P	R	F1	MCC	P	R	F1	MCC	P	R	F1	MCC	A
RF	0.79	0.13	0.22	0.13	0.40	0.98	0.57	0.22	0.00	0.00	0.00	-0.01	0.43
XGB	0.57	0.02	0.05	0.00	0.37	1.00	0.54	0.12	0.07	0.00	0.01	0.00	0.38
LSVM	0.75	0.02	0.03	0.04	0.37	1.00	0.54	0.08	0.00	0.00	0.00	0.00	0.37
RSVM	0.00	0.00	0.00	0.00	0.36	1.00	0.53	0.00	0.00	0.00	0.00	0.00	0.36
LDA	0.63	0.02	0.04	0.01	0.37	0.97	0.54	0.07	0.00	0.00	0.00	-0.04	0.37

P = Precision, R = Recall, MCC = Matthews Correlation Coefficient, A = Accuracy

Model performance during validation was substantially worse than during testing. As evidenced in Table 5 and Appendix III, all models exhibited strong bias towards the gap class, severely overclassifying this category. The Random Forest model showed some capability in classifying cane, albeit with poor accuracy. Weed detection was nearly absent across all models, with minimal pixel assignment to this class. Matthews Correlation Coefficient values reveal that most model-class combinations performed no better than random prediction, a finding corroborated by overall accuracy metrics indicating performance at or below chance level.

While Linear Discriminant Analysis performed best on the testing data, it was among the poorest-performing models during validation. Instead, Random Forest achieved the highest overall accuracy and Matthews Correlation Coefficient scores for both cane and gap classes. However, even this best-performing model exhibited systematic bias, overclassifying gaps and underclassifying cane, suggesting fundamental issues with model generalisability or feature representation.

3.3 Unsupervised classifier performance

3.3.1 Cluster labelling and ISODATA folding

Through comparison between the classified imagery and the supervised training data (Figure 7), unsupervised clusters were labelled and the seven original ISODATA clusters were folded into three classes. Table 6 summarises the mapping between model cluster numbers and final class labels. K-means and fuzzy c-means exhibit one-to-one mappings, whereas ISODATA produced multiple clusters per class label, reflecting its more granular clustering.

Table 6: Cluster labelling for unsupervised models

Model	Cane	Gaps	Weeds
k-means	Class 3	Class 1	Class 2
ISODATA	Class 1, 5, 6, 7	Class 2	Class 3, 4
c-means	Class 1	Class 2	Class 3

Labelling k-means and fuzzy c-means clusters was relatively straightforward. Clear spatial correspondence existed between clusters and training data for gap and cane classes, with the remaining cluster logically assigned to weed. However, ISODATA presented greater challenges due to less distinct cluster boundaries. Some clusters, such as cluster 4, overlapped multiple training classes, containing pixels within both gap and weed training polygons. For these ambiguous cases, majority voting determined the cluster label: clusters were assigned to the class containing the majority of their pixels within training polygons.

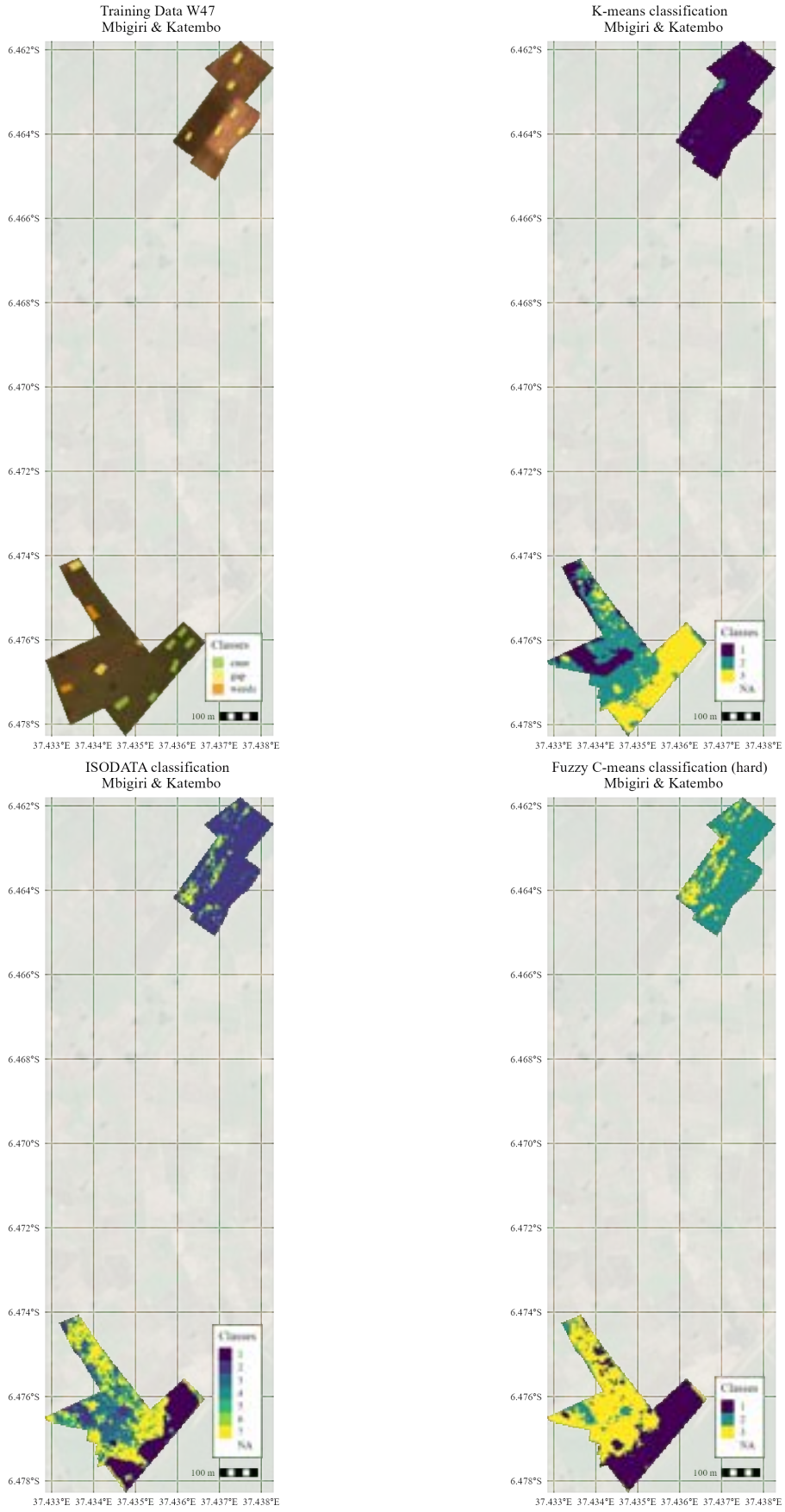

Figure 7: Comparison of unsupervised classifications, used for cluster labelling with training data from W47.

3.3.2 Validation performance

As with the supervised methods, comparison of unsupervised classifications against validation data provides robust insight into model performance. Table 7 summarises class-specific accuracy metrics and overall accuracy for each unsupervised model. Visualisations for the three models are presented in Appendix V.

Table 7: Validation performance by class, and model accuracy for unsupervised models.

	Cane				**Gaps**				**Weeds**				**Global**
Model	P	R	F1	MCC	P	R	F1	MCC	P	R	F1	MCC	A
k-means	0.72	0.02	0.04	0.03	0.71	0.90	0.79	0.66	0.07	0.73	0.13	0.10	0.38
ISODATA	0.87	0.37	0.52	0.33	0.83	0.82	0.82	0.72	0.07	0.48	0.12	0.04	0.54
c-means	0.75	0.02	0.05	0.05	0.75	0.90	0.82	0.70	0.07	0.74	0.13	0.09	0.38

P = Precision, R = Recall, MCC = Matthews Correlation Coefficient, A = Accuracy

Similarly to the supervised methods, unsupervised models performed poorly during validation, although the nature of the issues differed. Table 7 and Appendix V show that unsupervised models made a better distinction between gaps and vegetation. The gap class achieved relatively strong performance across all models, with good F1 scores and Matthews Correlation Coefficient values. However, overall model accuracies remained poor due to inadequate differentiation between cane and weeds. Models overclassified weeds and severely underclassified cane, resulting in low metrics for these classes. The ISODATA model was a partial exception, showing slightly improved cane classification compared to k-means and fuzzy c-means, but poorer weed classification.

Notably, looking at the fuzzy c-means confidence classification, where pixels with less than 75% confidence are classified as "unsure", some 90% of all pixels are found to be "unsure". Whilst the hard classification still assigns these pixels a class, seeing that the underlying confidence is widely lower than 75% highlights that there is model confusion.

The poor performance of both supervised and unsupervised models suggests fundamental issues with model generalisability, further explored in Section 4.

4 Discussion

4.1 Literature review

The literature review undertaken to answer SRQ1 demonstrates that gap and weed detection in sugarcane are relatively understudied topics, with the initial search query yielding only 42 records. Despite specifying "weeds" and "gaps", the vast majority of records focused on diseases, pests, and herbicides instead. Notably, most studies covered highly managed sugarcane farms in countries such as Australia, Brazil, and India, with minimal attention to East African countries—a broader trend observed in sugarcane research (Figueroa-Rodríguez et al., 2019; Santos et al., 2025). The absence of articles from Tanzania raises questions about generalisability, as methods and applications may not transfer uniformly across locations. For example, environmental moisture levels can influence soil reflectance (Lobell & Asner, 2002), potentially affecting spectral classification. Of the two records ultimately selected, one was a review paper covering many areas, while the other examined a study area in Brazil. When evaluating model performance further on in this section, it is important to note that these methods were not specifically developed for Tanzanian conditions.

In hindsight, the literature review was somewhat constrained, as evidenced by the limited number of records returned. For weed detection, the search could have been broadened to include other crops such as maize or soy, identifying additional weed detection methods. In addition, the literature review might be expanded through reference chaining, where the references of the identified articles are also checked, though this falls outside of the PRISMA framework and would move towards a so-called 'snowballing' methodology (Wohlin, 2014). While this might have raised applicability challenges for sugarcane, it would have enabled more targeted weed detection approaches than those employed in this research. On the other hand, the initial query could have been refined to better align with search criteria by explicitly excluding Unmanned Aerial Vehicle (UAV)-based approaches through the addition of "AND NOT 'UAV'" to the query string. This would have pre-emptively filtered many records that were instead removed during screening.

Finally, due to the limited scope of the literature review, certain PRISMA framework components were omitted. In particular, bias assessment was not performed. With only one author and without automation tools, comprehensive bias assessment would have been limited. However, individual authorship may introduce bias, particularly during record screening. As screening was based on title and abstract relevance to the research question, subjective judgement was unavoidable at this stage. While the aim was to maintain objectivity, records deemed irrelevant during screening may have had potential value. Most inappropriately screened records would likely have been filtered during eligibility assessment, though some relevant records may have been inadvertently excluded. Future iterations could benefit from more explicit screening criteria, such as specific keyword requirements.

Despite these limitations, the review successfully identified a substantial number of applicable methods, enabling continuation of the research and answering SRQ1. The PRISMA criteria effectively filtered records, and the framework provided a systematic, robust, and repeatable approach to identifying relevant methods.

4.2 Cloud filtering

During image preprocessing, as a precursor to addressing SRQ2 and SRQ3, cloud filtering was examined. PlanetScope's included cloud masking band (UDM) proved imperfect, remaining susceptible to wispy clouds and shadows. This finding is corroborated by broader research and highlights a weakness in the available data (Frazier & Hemingway, 2021). Conversely, despite reported accuracy, the applied OmniCloudMask exhibited severe bias, substantially overclassifying cloud presence at both spatial resolutions tested. While the model theoretically offers improved cloud masking with multiple cloud class detection, it lacks practical validation due to limited uptake and absence of comparative studies. Whether the method itself or its application in this research is flawed remains unclear. The similar overclassification at both 3 m and 9 m resolutions suggests the issue is not user error, though the lack of comparative studies weakens this conclusion. No definitive assessment is possible until broader research validates the method.

Alternative cloud masking methods or method combinations are available for exploration. While options developed specifically for PlanetScope imagery remain limited, several Sentinel-2 methods could potentially be adapted, though differences in spatial resolution may yield unexpected results (Bocharov et al., 2022; Magno et al., 2021). However, the desirability of pursuing more stringent cloud masking requires careful consideration from both scientific and practical perspectives, particularly regarding the trade-off between data quality and temporal coverage.

Scientifically, missing data from cloud masking can negatively impact kappa scores in satellite image time series classifications, though mitigation strategies exist (Y. Wang et al., 2026). Conversely, cloud contamination disrupts classification performance, as discussed in the methods section. From SmartCane's operational perspective, weekly reporting requirements create additional constraints. Extensive cloud filtering could result in consecutive weeks without usable imagery, preventing classification entirely and diminishing client value through prolonged information gaps. Given these considerations, only PlanetScope's UDM cloud mask was applied in this research, acknowledging its potential effects on results.

Cloud impacts warrant consideration, as wispy clouds and shadows are known to disrupt classification performance (Salberg, 2011). Because different bands are affected differently by clouds, normalised indices do not necessarily mitigate these effects (Julien & Sobrino, 2009). However, visual inspection during intermediate processing steps revealed minimal cloud-related issues. Cloud shadows were most frequently observed but did not appear to significantly influence classification results in these instances. While valid concerns exist regarding UDM limitations, operational requirements in a commercial context outweigh the need for more stringent cloud filtering at this stage. These potential limitations should be noted but do not require immediate remediation.

4.3 Training and validation data

As previously mentioned, field data collection was hampered by geopolitical constraints. The resulting lack of field data directly hindered the creation of quality training data and influenced model performance. Training data derived from limited field observations (which occasionally lacked temporal overlap with imagery), available imagery, and inferred seasonal trends provided a reasonable approximation but cannot be considered robust. Imagery interpretation is inherently subjective and susceptible to bias. Similarly, comparing pixel values to seasonal trend data is imperfect. While SmartCane colleagues agreed the training data provided reasonable approximations, substantial improvement is needed from a scientific perspective. Ideally, field visits would be expanded to establish a comprehensive data repository. Field data should prefer-

ably be collected as polygons rather than points to better align with satellite imagery's spatial characteristics. However, field data acquisition is often complicated or impractical. The current approximation methods were sufficient for this exploratory research, but improved training datasets could be generated through broader collaboration and diverse imagery sources. An approach similar to the expert validation process could be adopted, where multiple experts label imagery to create training data. This would reduce individual bias through majority or consensus voting systems, improving training data reliability.

Similarly, the validation data may contain bias or subjectivity. Despite utilising an established, scientifically supported framework, only two assessors participated. A larger assessor pool would reduce individual bias and minimise classification conflicts. During the consensus stage, numerous validation polygons showed mismatching classifications requiring resolution. Most conflicts involved distinguishing cane from weeds, highlighting the difficulty of visually differentiating these classes. This challenge was confirmed by the expert validators, who frequently expressed difficulty with certain areas and assigned "low" confidence ratings to many polygons.

Despite these limitations, the chosen approach represents the best available option given current constraints. Expert-based validation is an established method for situations where field data are inaccessible (Forestier et al., 2012; Wagner et al., 2025). While expanding the expert pool would reduce bias, identifying experts with experience in sugarcane classification from PlanetScope spectral indices is challenging due to the specialised nature of this work. Alternative methods such as DAMA (Baraldi et al., 2005) offer relative rather than absolute accuracy metrics, limiting their utility. The recommended path forward is to refine current training and validation strategies and incorporate field data as it becomes available.

4.4 Rates of change

The inclusion of rate of change calculations warrants consideration for future applications. Feature importance analysis reveals that rate of change bands are not particularly important in most models. However, the LDA model demonstrates that these bands exhibit lower collinearity than spectral indices, potentially proving valuable. Rate of change bands offer advantages because their range remains relatively stable, whereas absolute index values vary temporally and may confuse models (discussed in subsequent subsections). However, they introduce risk when images do not overlap due to cloud coverage or other factors, resulting in "NA" assignments. Some models, such as Random Forest, cannot handle missing data and will leave pixels unclassified, creating undesirable gaps in client-facing products.

Practically, rate of change bands currently provide valuable additional insights and should be retained as model refinement may increase their utility. For production implementation, a dual-model approach could mitigate NA-related issues: a primary model incorporating rate of change bands where available, and a reduced model for pixels lacking this information. This approach would be particularly relevant for Random Forest, as other models such as Extreme Gradient Boosting handle NA values natively.

4.5 Supervised classification for gap and weeds detection

Supervised classification methods for gap and weed detection yielded mixed results. Testing performance was generally strong, with Linear Discriminant Analysis (LDA) and Extreme Gradient Boosting (XGB) performing particularly well, achieving kappa scores of 0.83 and 0.79 respectively. Testing results demonstrate that distinguishing cane from gaps is feasible, with classification accuracies for these classes comparable to well-performing classification studies

(Lozano-Garzon et al., 2022). However, weed classification accuracy was consistently low, likely due to spectral signature similarities between cane and weeds. Poor weed classification during testing may also result from the spatial train-test split methodology. The testing dataset contained relatively few weed pixels, potentially biasing results given the substantially larger number of cane and gap pixels. While the stratified spatial split divided polygons 70/30, varying polygon sizes meant pixel counts did not follow this ratio. Nevertheless, testing results suggest that SRQ2 can be satisfactorily answered through application of either LDA or XGB models, as both accurately detect gaps. SRQ3 remains unanswerable based on the training data alone, as all models performed poorly on the weed class.

However, validation results suggest a different conclusion. Validation performance was poor across all classes and models, with overall accuracy scores below 0.43 and most Matthews Correlation Coefficient scores near zero, indicating performance no better than random assignment. This represents a poor outcome that compares unfavourably with similar studies (Lozano-Garzon et al., 2022; M. Wang et al., 2019). This raises the question of whether the models themselves are flawed or methodological shortcomings are responsible. While direct comparison between validation pixels and classified pixels technically constitutes non-probability sampling, limiting claims about accuracy across the entire mapped area (Olofsson et al., 2014), this is unlikely to be the primary cause of poor results. Given that validation imagery covered a substantial portion of the classified area, validation accuracies would likely not improve substantially with alternative sampling strategies such as systematic sampling (Congalton & Green, 2019). Instead, the underlying issue has been identified as domain shift between training and validation data. Principal Component Analysis (PCA) and t-Distributed Stochastic Neighbour Embedding (t-SNE) (Figure 8) reveal two fundamental problems in the data.

PCA analysis for both regions shows distinct clustering differences between red points (representing the training image, Week 47 mosaic) and blue points (representing validation imagery, Week 51 mosaic). For Mbigiri and Katembo, some cluster overlap exists, though most points are separated. For Moh, Shabani, and Yusuph fields, the clustering patterns show minimal overlap. Similarly, t-SNE plots reveal virtually no overlap between image clusters, with red and blue points remaining largely separated. These visualisations confirm severe domain shift, indicating that the datasets are fundamentally different (Soni et al., 2020).

This domain shift results from a critical shortcoming: training data were collected from only one week. While pixel values may appear similar to human observers, the actual values vary sufficiently to confuse the models. Training on a more diverse dataset encompassing multiple time points would likely introduce a broader range of pixel values and reduce inter-temporal differences. Alternative solutions include domain adaptation techniques such as unsupervised image statistics matching (Abramov et al., 2020) or randomised histogram matching (Yaras et al., 2023).

Drawing robust conclusions about SRQ2 and SRQ3 based on supervised classifiers is challenging given the substantial discrepancy between training and validation results. Nevertheless, training results clearly demonstrate that distinguishing sugarcane from gaps or bare soil is feasible, with Extreme Gradient Boosting and Linear Discriminant Analysis models performing best. However, weed identification was not achieved with any model, likely due to spectral similarities between sugarcane and weeds. The poor validation performance likely stems from domain shift rather than model inadequacy. Before practical application, the workflow requires modification to address domain shift through either time-series training data or domain adaptation techniques.

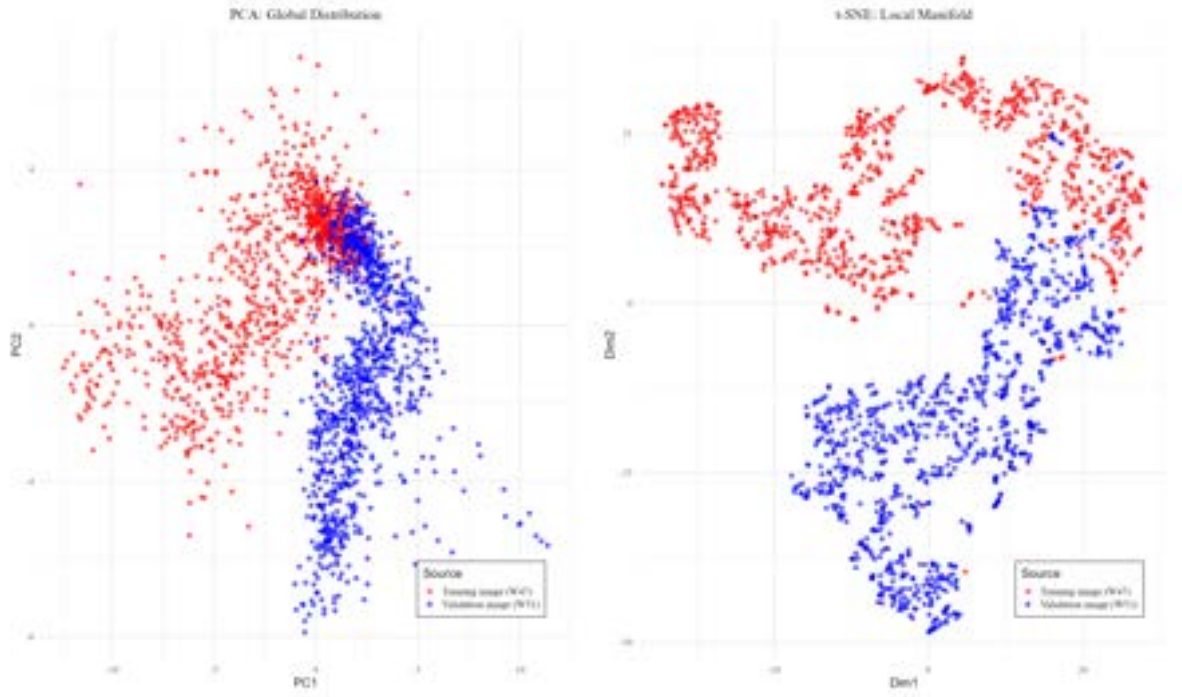

(a) PCA and t-SNE plots for fields Mbigiri & Katembo

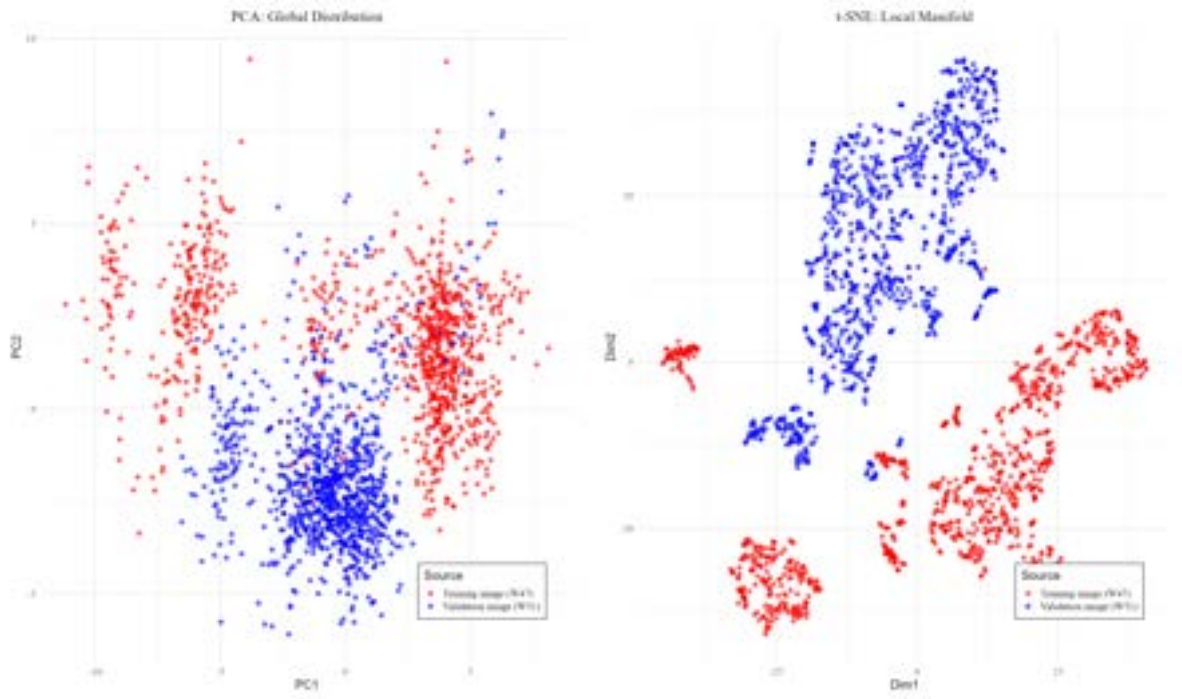

(b) PCA and t-SNE plots for fields Moh, Shabani & Yusuph

Figure 8: PCA and t-SNE plots for training data (Week 47) and validation data (Week 51)

4.6 Unsupervised classification for gap and weeds detection

Similar to supervised classifications, unsupervised classifications present mixed results. Although accuracy metrics could not be calculated for unsupervised model training data, visual comparison with training polygons during cluster labelling suggested reasonable performance. Figure 7 shows realistic spatial patterns aligning well with training data, and cluster labelling was relatively straightforward, except for some ISODATA confusion between weeds and other classes. Performance appeared stronger for sugarcane and gaps, with weeds causing confusion, mirroring supervised model behaviour. This suggests that while these models may distinguish vegetation from gaps, inter-vegetation classification (sugarcane versus weeds) remains challenging. Although this conclusion is based on subjective interpretation during cluster labelling rather than quantitative metrics, unsupervised models have demonstrated strong performance in similar classification tasks (Everingham et al., 2007; Nihar et al., 2022).

Overall validation performance was poor, comparable to supervised models but with marginally higher global accuracies. Class-specific metrics revealed differences, with generally better performance for sugarcane and gaps. Gaps achieved relatively high Matthews Correlation Coefficient values, indicating reliable prediction. These findings further support the conclusion that distinguishing vegetation from gaps is achievable, while discriminating between sugarcane and weeds remains difficult. These results are also affected by the previously identified domain shift; addressing this issue should improve model performance.

Alternative unsupervised classifiers could improve results, assuming the domain shift is addressed. If time-series imagery is adopted as training data, parallelised inter-image k-means algorithms could be explored (Han & Lee, 2023). Additionally, spatio-contextual fuzzy c-means models incorporating spatial information alongside spectral data have demonstrated promising results (Subudhi et al., 2013; J. Xu et al., 2019, 2020). These spatial approaches may prove particularly valuable for weed detection, as weeds typically exhibit spatial clustering patterns.

Similar to supervised methods, drawing robust conclusions about SRQ2 and SRQ3 is challenging given the domain shift issue. Nevertheless, unsupervised models show promise. ISODATA in particular achieved the relative best performance for classifying sugarcane and gaps, though weed classification remained poor. Again, the distinction between vegetation and gaps appears achievable, while discriminating between sugarcane and weeds proves more difficult.

4.7 Closing discussion points

Beyond literature and model results, practical workflow considerations merit discussion. A key question is whether a single three-class classifier is optimal. While this approach was adopted for this exploratory research, it may not represent the most effective workflow. Models demonstrated promising results for distinguishing gaps from vegetation, but struggled with inter-vegetation classification (cane versus weeds). A sequential classification approach may prove more appropriate: a first model optimised for binary gap-vegetation classification, followed by a second model for vegetation type classification. This would enable greater model specificity at each stage. That being said, alternative methodologies also warrant consideration. Although deep learning was excluded from the literature review due to typical data volume requirements, unsupervised deep learning methods merit exploration (Van Strien & Grêt-Regamey, 2022). Should additional training data become available, models employing long short-term memory architectures could prove valuable (Lake et al., 2022). This exploratory research focused on a subset of available methods rather than providing exhaustive coverage, establishing a foundation for future methodological exploration.

5 Conclusion & Recommendations

5.1 Scientific perspective

This research explored available methods for automated gap and weed detection during sugarcane emergence in Tanzania's Morogoro region using PlanetScope imagery, successfully addressing this objective. A systematic literature review using the PRISMA framework enabled answering SRQ1, identifying a range of applicable methods and knowledge for gap and weed detection. While minor improvements in bias prevention could be made, the review provided a solid foundation for method selection.

Five supervised and three unsupervised classification models were developed using 14 spectral indices from PlanetScope imagery and 14 additional bands representing weekly index changes, based on the literature review and expertise from the host organisation. Training data quality for supervised methods was limited, potentially introducing bias. Future work should prioritise acquiring high-quality training data through field collection or expert knowledge aggregation, as demonstrated during validation in this research.

Supervised models, particularly Extreme Gradient Boosting and Linear Discriminant Analysis, demonstrated strong potential for classifying gaps versus vegetation when tested on spatial hold-out sets. However, inter-vegetation classification (cane versus weeds) proved challenging. Validation against independent data did not yield additional insights due to domain shift between training and validation datasets, which must be addressed before drawing definitive conclusions. Unsupervised methods, particularly ISODATA, showed promise with reasonable performance for gap and cane classes despite domain shift effects that severely impacted supervised methods.

While SRQ2 and SRQ3 cannot be definitively answered due to training data limitations and validation domain shift, results indicate that multiple models (both supervised and unsupervised) hold promise for accurately identifying gaps during sugarcane emergence. Differentiating sugarcane from weeds remains challenging, warranting further investigation of alternative models. Several promising methods have been identified, though no clear consensus exists as their application to sugarcane remains limited compared to other crops and contexts.

Finally, cloud cover influence warrants consideration. Cloud masking methodology significantly affects model results. Conservative masking may leave wispy clouds and shadows that interfere with spectral signatures, while overly aggressive masking causes data decimation, leaving insufficient data for analysis. Balancing these trade-offs is essential for operational implementation.

5.2 Practical perspective

For the host organisation, these findings lead to the recommendation to further develop models before operational implementation. Despite noted shortcomings, the promising results indicate that well-functioning models would provide substantial value. The relatively strong performance of ISODATA warrants prioritisation for further development.

Development priorities should include creating multi-week training datasets collaboratively with expert teams and, if possible, field data collection to support the development of supervised models. To address domain shift in supervised and unsupervised models, the models should be trained on time-series data rather than single-week mosaics, or domain adaptation techniques such as histogram matching or statistics matching should be applied. Cloud masking methodology requires careful consideration. The organisation would benefit from a well-characterised

cloud masking model with documented accuracy tailored to PlanetScope imagery, a potentially valuable future project as cloud interference will likely also affect other development projects, as well as current workflows.

Practical integration considerations must also be addressed, as models have applicability only during specific growth cycle windows. Applying methods based on field age appears appropriate, though the precise growth cycle range where models add value requires further exploration and monitoring.

While this research does not deliver a fully operational product ready for immediate implementation, it represents a crucial first step. Multiple promising methods have been identified, and practical recommendations are provided for their implementation alongside considerations for future research to improve model functionality or explore alternative approaches entirely.

References

Abdi, A. M. (2019). Land cover and land use classification performance of machine learning algorithms in a boreal landscape using sentinel-2 data. *GIScience Remote Sensing*, *57*(1), 1–20. https://doi.org/10.1080/15481603.2019.1650447

Abramov, A., Bayer, C., & Heller, C. (2020). Keep it Simple: Image Statistics Matching for Domain Adaptation. *arXiv (Cornell University)*. https://doi.org/10.48550/arxiv.2005.12551

Achon, M. A., Serrano, L., Clemente-Orta, G., & Sossai, S. (2016). First Report of Maize chlorotic mottle virus on a Perennial Host, Sorghum halepense, and Maize in Spain. *Plant Disease*, *101*(2), 393. https://doi.org/10.1094/pdis-09-16-1261-pdn

Ajayi, O. G., Ibrahim, P. O., & Adegboyega, O. S. (2024). Effect of hyperparameter tuning on the performance of YOLOV8 for multi crop classification on UAV images. *Applied Sciences*, *14*(13), 5708. https://doi.org/10.3390/app14135708

Baraldi, A., Bruzzone, L., & Blonda, P. (2005). Quality assessment of classification and cluster maps without ground truth knowledge. *IEEE Transactions on Geoscience and Remote Sensing*, *43*(4), 857–873. https://doi.org/10.1109/tgrs.2004.843074

Bhatt, R., Hossain, A., Majumder, D., Chandra, M. S., Ghimire, R., Shahzad, M. F., Verma, K. K., Riar, A. S., Rajput, V. D., Oliveira, M. W., Nisi, A., Almalki, R. S., Bárek, V., Brestic, M., & Maitra, S. (2024). Prospects of artificial intelligence for the sustainability of sugarcane production in the modern era of climate change: An overview of related global findings. *Journal of Agriculture and Food Research*, *18*, 101519. https://doi.org/10.1016/j.jafr.2024.101519

Bocharov, D. A., Nikolaev, D. P., Pavlova, M. A., & Timofeev, V. A. (2022). Cloud shadows detection and compensation algorithm on multispectral satellite images for agricultural regions. *Journal of Communications Technology and Electronics*, *67*(6), 728–739. https://doi.org/10.1134/s1064226922060171

Cappelini, L. T. D., Cordeiro, D., Brondi, S. H. G., Prieto, K. R., & Vieira, E. M. (2012). Development of methodology for determination of pesticides residue in water by SPE/HPLC/DAD. *Environmental Technology*, *33*(20), 2299–2304. https://doi.org/10.1080/09593330.2012.665494

Chen, M., Wang, Q., & Li, X. (2018). Discriminant Analysis with Graph Learning for Hyperspectral Image Classification. *Remote Sensing*, *10*(6), 836. https://doi.org/10.3390/rs10060836

Chen, T., He, T., Benesty, M., Khotilovich, V., Tang, Y., Cho, H., Chen, K., Mitchell, R., Cano, I., Zhou, T., Li, M., Xie, J., Lin, M., Geng, Y., Li, Y., & Yuan, J. (2025). *Xgboost: Extreme gradient boosting* [R package version 1.7.11.1]. https://doi.org/10.32614/CRAN.package.xgboost

Chicco, D., & Jurman, G. (2020). The advantages of the Matthews correlation coefficient (MCC) over F1 score and accuracy in binary classification evaluation. *BMC Genomics*, *21*(1), 6. https://doi.org/10.1186/s12864-019-6413-7

Congalton, R. G., & Green, K. (2019, August). *Assessing the accuracy of remotely sensed data*. https://doi.org/10.1201/9780429052729

Conrad, O., Bechtel, B., Bock, M., Dietrich, H., Fischer, E., Gerlitz, L., Wehberg, J., Wichmann, V., & Böhner, J. (2015). System for automated geoscientific analyses (saga) v. 2.1.4. *Geoscientific model development*, *8*(7), 1991–2007. https://doi.org/10.5194/gmd-8-1991-2015

De Araújo, T. R., De Assis Dos Santos Diniz, F., Mendes, B. L., Almeida, L. C., & Santiago, T. R. (2025). Pratylenchus zeae is the main root lesion nematode affecting sugarcane in the world's most important producing regions. *Physiological and Molecular Plant Pathology*, *136*, 102576. https://doi.org/10.1016/j.pmpp.2025.102576

De Assis, A. P., Okumura, L. L., Saczk, A. A., & De Oliveira, M. F. (2013). New Voltammetry-Based technique for the determination of tebuthiuron in crystal and brown sugar samples. *Journal of the Brazilian Chemical Society*. https://doi.org/10.5935/0103-5053.20130264

De Oliveira Maia, F. C., Bufon, V. B., & Leão, T. P. (2022). Vegetation indices as a Tool for Mapping Sugarcane Management Zones. *Precision Agriculture*, *24*(1), 213–234. https://doi.org/10.1007/s11119-022-09939-7

De Souza, M. F., Amaral, L. R. D., De Medeiros Oliveira, S. R., Coutinho, M. A. N., & Netto, C. F. (2019). Spectral differentiation of sugarcane from weeds. *Biosystems Engineering*, *190*, 41–46. https://doi.org/10.1016/j.biosystemseng.2019.11.023

Demirhan, H. (2024). Mixed fuzzy c-means clustering. *Information Sciences*, *690*, 121528. https://doi.org/10.1016/j.ins.2024.121528

Deng, G., Zhou, F., Dong, H., Xu, Z., & Li, Y. (2025). Accurate sugarcane detection and row fitting using SugarRow-YOLO and Clustering-Based SPLine methods for autonomous agricultural operations. *Applied Sciences*, *15*(14), 7789. https://doi.org/10.3390/app15147789

d'Errico, A., Peraza, S., Weiss, I., Martinez, W., Monge, E. A., Wouters, I. M., Wegman, D. H., Jakobsson, K., & Kromhout, H. (2025). Occupational exposure to respirable and inhalable dust and its components in a Nicaraguan sugarcane plantation. *Occupational and Environmental Medicine*, *82*(1), 36–43. https://doi.org/10.1136/oemed-2024-109604

Di Girolamo-Neto, C., Sanches, I. D., Neves, A. K., Prudente, V. H. R., Körting, T. S., Picoli, M. C. A., & De Aragão, L. E. O. E. C. (2019). Assessment of Texture Features for Bermudagrass (Cynodon dactylon) Detection in Sugarcane Plantations. *Drones*, *3*(2), 36. https://doi.org/10.3390/drones3020036

Dunn, J. C. (1973). A fuzzy relative of the isodata process and its use in detecting compact well-separated clusters. *Journal of Cybernetics*, *3*(3), 32–57. https://doi.org/10.1080/01969727308546046

Everingham, Y. L., Lowe, K. H., Donald, D. A., Coomans, D. H., & Markley, J. (2007). Advanced satellite imagery to classify sugarcane crop characteristics. *Agronomy for Sustainable Development*, *27*(2), 111–117. https://doi.org/10.1051/agro:2006034

Ferreira, R., Contato, E., Kuva, M., Ferraudo, A., Alves, P., Magario, F., & Salgado, T. (2011). Organization of weed communities in sugarcane standard groupings. *Planta Daninha*, *29*(2), 364–371.

Figueroa-Rodríguez, K. A., Hernández-Rosas, F., Figueroa-Sandoval, B., Velasco-Velasco, J., & Rivera, N. A. (2019). What has been the focus of sugarcane research? A bibliometric overview. *International Journal of Environmental Research and Public Health*, *16*(18), 3326. https://doi.org/10.3390/ijerph16183326

Forestier, G., Puissant, A., Wemmert, C., & Gançarski, P. (2012). Knowledge-based region labeling for remote sensing image interpretation. *Computers Environment and Urban Systems*, *36*(5), 470–480. https://doi.org/10.1016/j.compenvurbsys.2012.01.003

Frazier, A. E., & Hemingway, B. L. (2021). A technical review of planet smallsat data: Practical considerations for processing and using planetscope imagery. *Remote Sensing*, *13*(19), 3930. https://doi.org/10.3390/rs13193930

Gawlikowski, J., Ebel, P., Schmitt, M., & Zhu, X. X. (2022). Explaining the effects of clouds on remote sensing scene classification. *IEEE Journal of Selected Topics in Applied Earth Observations and Remote Sensing*, *15*, 9976–9986. https://doi.org/10.1109/jstars.2022.3221788

Gell, G., Sebestyén, E., & Balázs, E. (2014). Recombination analysis of Maize dwarf mosaic virus (MDMV) in the Sugarcane mosaic virus (SCMV) subgroup of potyviruses. *Virus Genes*, *50*(1), 79–86. https://doi.org/10.1007/s11262-014-1142-0

Gitelson, A., & Merzlyak, M. N. (1994). Quantitative estimation of chlorophyll-a using reflectance spectra: Experiments with autumn chestnut and maple leaves. *Journal of Photochemistry and Photobiology B Biology*, *22*(3), 247–252. https://doi.org/10.1016/1011-1344(93)06963-4

Gitelson, A. A., Gritz, Y., & Merzlyak, M. N. (2003). Relationships between leaf chlorophyll content and spectral reflectance and algorithms for non-destructive chlorophyll assessment in higher plant leaves. *Journal of Plant Physiology*, *160*(3), 271–282. https://doi.org/10.1078/0176-1617-00887

Gitelson, A. A., Kaufman, Y. J., & Merzlyak, M. N. (1996). Use of a green channel in remote sensing of global vegetation from EOS-MODIS. *Remote Sensing of Environment*, *58*(3), 289–298. https://doi.org/10.1016/s0034-4257(96)00072-7

Gitelson, A. A., Kaufman, Y. J., Stark, R., & Rundquist, D. (2002). Novel algorithms for remote estimation of vegetation fraction. *Remote Sensing of Environment*, *80*(1), 76–87. https://doi.org/10.1016/s0034-4257(01)00289-9

Han, S., & Lee, J. (2023). Parallelized Inter-Image K-Means clustering algorithm for unsupervised classification of series of satellite images. *Remote Sensing*, *16*(1), 102. https://doi.org/10.3390/rs16010102

Heil, J., Häring, V., Marschner, B., & Stumpe, B. (2018). Advantages of fuzzy k-means over k-means clustering in the classification of diffuse reflectance soil spectra: A case study with West African soils. *Geoderma*, *337*, 11–21. https://doi.org/10.1016/j.geoderma.2018.09.004

Hijmans, R. J. (2025). *Terra: Spatial data analysis* [R package version 1.8-54]. https://doi.org/10.32614/CRAN.package.terra

Huete, A., Didan, K., Miura, T., Rodriguez, E., Gao, X., & Ferreira, L. (2002). Overview of the radiometric and biophysical performance of the MODIS vegetation indices. *Remote Sensing of Environment*, *83*(1-2), 195–213. https://doi.org/10.1016/s0034-4257(02)00096-2

Hussain, S., Khaliq, A., Mehmood, U., Qadir, T., Saqib, M., Iqbal, M. A., & Hussain, S. (2019, February). *Sugarcane Production under Changing Climate: Effects of Environmental Vulnerabilities on Sugarcane Diseases, Insects and Weeds*. https://doi.org/10.5772/intechopen.81131

Jeyaraman, A., Babulal, S. M., Chen, T.-W., Sengodan, S., Yu, J., Chen, S.-M., & Juang, R.-S. (2025). In-situ construction of WO3 nanorods on the carbon microsphere composite for effective electrochemical determination of mesotrione herbicide in environmental samples. *Journal of the Taiwan Institute of Chemical Engineers*, *174*, 106226. https://doi.org/10.1016/j.jtice.2025.106226

Johansen, K., Sallam, N., Robson, A., Samson, P., Chandler, K., Derby, L., Eaton, A., & Jennings, J. (2017). Using GeoEYE-1 imagery for Multi-Temporal Object-Based detection of canegrub damage in sugarcane fields in Queensland, Australia. *GIScience Remote Sensing*, *55*(2), 285–305. https://doi.org/10.1080/15481603.2017.1417691

Johnson, R. M., Orgeron, A. J., Spaunhorst, D. J., Huang, I.-S., & Zimba, P. V. (2023). Discrimination of weeds from sugarcane in Louisiana using hyperspectral leaf reflectance data and pigment analysis. *Weed Technology*, *37*(2), 123–131. https://doi.org/10.1017/wet.2023.14

Julien, Y., & Sobrino, J. A. (2009). Comparison of cloud-reconstruction methods for time series of composite NDVI data. *Remote Sensing of Environment*, *114*(3), 618–625. https://doi.org/10.1016/j.rse.2009.11.001

Karthik, N., & Shivakumar, B. R. (2021, January 1). *Land cover mapping capability of chain-cluster, k-means, and isodata techniques—a case study*. https://doi.org/10.1007/978-981-16-0443-0_23

Kaufman, Y., & Tanre, D. (1992). Atmospherically resistant vegetation index (ARVI) for EOS-MODIS. *IEEE Transactions on Geoscience and Remote Sensing*, *30*(2), 261–270. https://doi.org/10.1109/36.134076

Khuc, T. D., Luong, N. D., Dang, D. H., & Tran, V. A. (2025). Comparison of random forest and extreme gradient boosting algorithms in land cover classification in van yen district, yen bai province, vietnam. *Journal of Hydro-meteorology*, *06*(23), 50–59. https://doi.org/10.36335/vnjhm.2025(23).50-59

Kong, C.-Y., Wickramasinghe, K. P., Xu, C.-H., Mao, J., Liu, H.-B., Kumar, T., Lin, X.-Q., Li, X.-J., Tian, C.-Y., Zhao, P.-F., & Lu, X. (2025). Recent advances in sugarcane leaf scald Disease: Pathogenic insights and sustainable management approaches. *Plants*, *14*(4), 508. https://doi.org/10.3390/plants14040508

Kuhn & Max. (2008). Building predictive models in r using the caret package. *Journal of Statistical Software*, *28*(5), 1–26. https://doi.org/10.18637/jss.v028.i05

Lake, T. A., Runquist, R. D. B., & Moeller, D. A. (2022). Deep learning detects invasive plant species across complex landscapes using Worldview-2 and Planetscope satellite imagery. *Remote Sensing in Ecology and Conservation*, *8*(6), 875–889. https://doi.org/10.1002/rse2.288

Li, Y., Guo, J., Lin, L., Guo, H., & Yang, F. (2024). A color-changed fluorescence sensor for pesticide triclopyr 2-butoxyethyl ester based on naphthalimide Schiff-base. *Journal of Photochemistry and Photobiology A Chemistry*, *457*, 115894. https://doi.org/10.1016/j.jphotochem.2024.115894

Lloyd, S. (1982). Least squares quantization in pcm. *IEEE Transactions on Information Theory*, *28*(2), 129–137. https://doi.org/10.1109/tit.1982.1056489

Lobell, D., & Asner, G. (2002). Moisture Effects on Soil Reflectance. *Soil Science Society of America*, *66*(3). https://doi.org/10.2136/sssaj2002.7220

Louhaichi, M., Borman, M. M., & Johnson, D. E. (2001). Spatially located platform and aerial photography for documentation of grazing impacts on wheat. *Geocarto International*, *16*(1), 65–70. https://doi.org/10.1080/10106040108542184

Lozano-Garzon, C., Bravo-Cordoba, G., Castro, H., Gonzalez-Rodriguez, G., Nino, D., Nunez, H., Pardo, C., Vivas, A., Castro, Y., Medina, J., Motta, L. C., Rojas, J. R., & Suarez, L. I. (2022). Remote sensing and machine learning modeling to support the identification of sugarcane crops. *IEEE Access*, *10*, 17542–17555. https://doi.org/10.1109/access.2022.3148691

Luciano, A. C. D. S., Picoli, M. C. A., Rocha, J. V., Franco, H. C. J., Sanches, G. M., Leal, M. R. L. V., & Maire, G. L. (2018). Generalized space-time classifiers for monitoring sugarcane areas in brazil. *Remote Sensing of Environment*, *215*, 438–451. https://doi.org/10.1016/j.rse.2018.06.017

Magno, R., Rocchi, L., Dainelli, R., Matese, A., di Gennaro, S., Chen, C., Son, N., & Toscano, P. (2021). AgroShadow: A New Sentinel-2 Cloud Shadow Detection Tool for Precision Agriculture. *Remote Sensing*, *13*(6). https://doi.org/10.3390/rs13061219

Mahadea-Nemdharry, R., Doorga, J. R., Busawon, K., & Seeruttun, S. (2025). Enhancing sugarcane field management in a tropical island: A comparative analysis of mapping gaps in sugarcane fields using drone and satellite imageries. *Remote Sensing Applications Society and Environment*, 101570. https://doi.org/10.1016/j.rsase.2025.101570

Maldaner, L. F., Molin, J. P., Martello, M., Tavares, T. R., & Dias, F. L. (2021). Identification and measurement of gaps within sugarcane rows for site-specific management: Comparing different sensor-based approaches. *Biosystems Engineering*, *209*, 64–73. https://doi.org/10.1016/j.biosystemseng.2021.06.016

Maldaner, L. F., Molin, J. P., Canata, T. F., & Martello, M. (2021). A system for plant detection using sensor fusion approach based on machine learning model. *Computers and Electronics in Agriculture*, *189*, 106382. https://doi.org/10.1016/j.compag.2021.106382

Maldaner, L., Molin, J., dos Santos Dias, C., & da Silva, E. (2025). When ratoon longevity matters: Spatial and temporal analysis of sugarcane plant population patterns using features extracted from UAV images. *Remote Sensing Applications: Society and Environment*, *39*(101703). https://doi.org/10.1016/j.rsase.2025.101703

McCarthy, C., Rees, S., & Baillie, C. (2009). Machine vision-based weed spot spraying: a review and where next for sugarcane? *Proceedings of the 32nd Annual Conference of the Australian Society of Sugar Cane Technologists*, *32*, 424–432. https://research.usq.edu.au/item/9zx5w/machine-vision-based-weed-spot-spraying-a-review-and-where-next-for-sugarcane

McFeeters, S. K. (1996). The use of the normalized difference water index (ndwi) in the delineation of open water features. *International Journal of Remote Sensing*, *17*(7), 1425–1432. https://doi.org/10.1080/01431169608948714

Melgani, F., & Bruzzone, L. (2004). Classification of hyperspectral remote sensing images with support vector machines. *IEEE Transactions on Geoscience and Remote Sensing*, *42*(8), 1778–1790. https://doi.org/10.1109/tgrs.2004.831865

Mellor, A., Boukir, S., Haywood, A., & Jones, S. (2015). Exploring issues of training data imbalance and mislabelling on random forest performance for large area land cover classification using the ensemble margin. *ISPRS Journal of Photogrammetry and Remote Sensing*, *105*, 155–168. https://doi.org/10.1016/j.isprsjprs.2015.03.014

Meng, J.-Y., Ntambo, M. S., Luo, L.-M., Huang, M.-T., Fu, H.-Y., & Gao, S.-J. (2019). Molecular identification of Xanthomonas albilineans infecting elephant grass (Pennisetum purpureum) in China. *Crop Protection*, *124*, 104853. https://doi.org/10.1016/j.cropro.2019.104853

Meyer, D., Dimitriadou, E., Hornik, K., Weingessel, A., & Leisch, F. (2024). *E1071: Misc functions of the department of statistics, probability theory group (formerly: E1071), tu wien* [R package version 1.7-16]. https://doi.org/10.32614/CRAN.package.e1071

Mgode, G. F., Japhary, M. M., Mhamphi, G. G., Kiwelu, I., Athaide, I., & Machang'u, R. S. (2019). Leptospirosis in sugarcane plantation and fishing communities in Kagera northwestern Tanzania. *PLoS neglected tropical diseases*, *13*(5), e0007225. https://doi.org/10.1371/journal.pntd.0007225

Mielke, K. C., Da Silva Brochado, M. G., Laube, A. F. S., Guimarães, T., De Paula Medeiros, B. A., & Mendes, K. F. (2023). Pyrolysis Temperature vs. Application Rate of Biochar Amendments: Impacts on Soil Microbiota and Metribuzin Degradation. *International Journal of Molecular Sciences*, *24*(13), 11154. https://doi.org/10.3390/ijms241311154

Moazzam, S. I., Khan, U. S., Qureshi, W. S., Tiwana, M. I., Rashid, N., Alasmary, W. S., Iqbal, J., & Hamza, A. (2021). A Patch-Image based classification approach for detection of weeds in sugar beet crop. *IEEE Access*, *9*, 121698–121715. https://doi.org/10.1109/access.2021.3109015

Msomba, B. H., Ndaki, P. M., & Joseph, C. O. (2024). Sugarcane sustainability in a changing climate: a systematic review on pests, diseases, and adaptive strategies. *Frontiers in Agronomy*, *6*. https://doi.org/10.3389/fagro.2024.1423233

Nakhone, W., Ndiema, A., & Akundabweni, L. (2025). The role of farmer groups in the adoption of sustainable sugarcane farming practices in Kakamega North sub-county. *The Strategic Journal of Business Change Management*, *12*(2), 1458–1470.

Nihar, A., Patel, N. R., Pokhariyal, S., & Danodia, A. (2022). Sugarcane crop type discrimination and area mapping at field scale using sentinel images and machine learning methods. *Journal of the Indian Society of Remote Sensing*, *50*(2), 217–225. https://doi.org/10.1007/s12524-021-01444-0

Olofsson, P., Foody, G. M., Herold, M., Stehman, S. V., Woodcock, C. E., & Wulder, M. A. (2014). Good practices for estimating area and assessing accuracy of land change. *Remote Sensing of Environment*, *148*, 42–57. https://doi.org/10.1016/j.rse.2014.02.015

Page, M. J., McKenzie, J. E., Bossuyt, P. M., Boutron, I., Hoffmann, T. C., Mulrow, C. D., Shamseer, L., Tetzlaff, J. M., Akl, E. A., Brennan, S. E., Chou, R., Glanville, J., Grimshaw, J. M., Hróbjartsson, A., Lalu, M. M., Li, T., Loder, E. W., Mayo-Wilson, E., McDonald, S., ... Moher, D. (2021). The PRISMA 2020 statement: an updated guideline for reporting systematic reviews. *BMJ*, n71. https://doi.org/10.1136/bmj.n71

Paleti, L., Nagasri, A., Sunitha, P., Sandya, V., & Sumallika, T. (2023). SUGAR CANE LEAF DISEASE CLASSIFICATION AND IDENTIFICATION USING DEEP MACHINE LEARNING ALGORITHMS. *Journal of Theoretical and Applied Information Technology*, *101*(20), 6460–6472.

Panduangnat, L., Posom, J., Saikaew, K., Phuphaphud, A., Wongpichet, S., Chinapas, A., Sukpancharoen, S., & Saengprachatanarug, K. (2024). Time-efficient low-resolution RGB aerial imaging for precision mapping of weed types in site-specific herbicide application. *Crop Protection*, *184*, 106805. https://doi.org/10.1016/j.cropro.2024.106805

Patel, D., Patel, R., Station, M. S. R., & University, N. A. (2014). *INFLUENCE OF SETT SIZE, SEED RATE AND SETT TREATMENT ON YIELD AND QUALITY OF SUGARCANE* (tech. rep. No. 1). https://www.researchgate.net/profile/Darpana-Patel-2/publication/350515357_N_Save_Nature_to_Survive_INFLUENCE_OF_SETT_SIZE_SEED_RATE_AND_SETT_TREATMENT_ON_YIELD_AND_QUALITY_OF_SUGARCANE/links/60644cf0458515e83482739b/N-Save-Nature-to-Survive-INFLUENCE-OF-SETT-SIZE-SEED-RATE-AND-SETT-TREATMENT-ON-YIELD-AND-QUALITY-OF-SUGARCANE.pdf

Pawley, S. (2024). *Rsagacmd: Linking r with the open-source 'saga-gis' software* [R package version 0.4.3]. https://doi.org/10.32614/CRAN.package.Rsagacmd

Pearce, W. (1985). Cloud shadow effects on remote sensing. *IEEE Transactions on Geoscience and Remote Sensing*, *GE-23*(5), 634–639. https://doi.org/10.1109/tgrs.1985.289381

Pebesma, E. (2018). Simple Features for R: Standardized Support for Spatial Vector Data. *The R Journal*, *10*(1), 439–446. https://doi.org/10.32614/RJ-2018-009

Pereira, R. M., Casaroli, D., Vellame, L. M., Júnior, J. A., Evangelista, A. W. P., & Battisti, R. (2020). Water deficit detection in sugarcane using canopy temperature from satellite images. *Australian Journal of Crop Science*, (14(03):2020), 400–407. https://doi.org/10.21475/ajcs.20.14.03.p1647

Pirotti, F., Sunar, F., & Piragnolo, M. (2016). Benchmark of machine learning methods for classification of a sentinel-2 image. *The international archives of the photogrammetry, remote sensing and spatial information sciences/International archives of the photogrammetry, remote sensing and spatial information sciences*, *XLI-B7*, 335–340. https://doi.org/10.5194/isprs-archives-xli-b7-335-2016

Planet Labs Inc. (2021). *PlanetScope Product Specifications* (tech. rep.).

Ploton, P., Mortier, F., Réjou-Méchain, M., Barbier, N., Picard, N., Rossi, V., Dormann, C., Cornu, G., Viennois, G., Bayol, N., Lyapustin, A., Gourlet-Fleury, S., & Pélissier, R. (2020). Spatial validation reveals poor predictive performance of large-scale ecological mapping models. *Nature Communications*, *11*(1), 4540. https://doi.org/10.1038/s41467-020-18321-y

Priyadarshini, K. N., Kumar, M., Rahaman, S. A., & Nitheshnirmal, S. (2018). A comparative study of advanced land use/land cover classification algorithms using sentinel-2 data. *The international archives of the photogrammetry, remote sensing and spatial information sciences*, *XLII-5*, 665–670. https://doi.org/10.5194/isprs-archives-xlii-5-665-2018

Qi, J., Chehbouni, A., Huete, A., Kerr, Y., & Sorooshian, S. (1994). A modified soil adjusted vegetation index. *Remote Sensing of Environment*, *48*(2), 119–126. https://doi.org/10.1016/0034-4257(94)90134-1

R Core Team. (2025). *R: A language and environment for statistical computing*. R Foundation for Statistical Computing. Vienna, Austria. https://www.R-project.org/

Rao, G., Mall, S., Raj, S., & Snehi, S. (2011). Review article: Phytoplasma diseases affecting various plant species in India. *Acta Phytopathologica et Entomologica Hungarica*, *46*(1), 59–99. https://doi.org/10.1556/aphyt.46.2011.1.7

Rao, G. P. (2021). Our understanding about phytoplasma research scenario in India. *Indian Phytopathology*, *74*(2), 371–401. https://doi.org/10.1007/s42360-020-00303-1

Rashmi, C., Chaluvaiah, S., & Kumar, G. H. (2016). An efficient parallel block processing approach for k -means algorithm for high resolution orthoimagery satellite images. *Procedia Computer Science*, *89*, 623–631. https://doi.org/10.1016/j.procs.2016.06.025

Ratchawang, S., Chotpantarat, S., & Charoenrojying, P. (2022). Assessment of atrazine migration in soil and groundwater using nitrate as an indicator in an intensively cultivated sugarcane field, Suphan Buri Province, Thailand. *Frontiers in Earth Science*, *10*. https://doi.org/10.3389/feart.2022.855599

Rathika, S., Ramesh, T., & Jagadeesan, R. (2023). Weed management in sugarcane: A review. *The Pharma Innovation*, *12*(6), 3883–3887.

Rihan, M., Talukdar, S., Naikoo, M. W., Islam, M. R., Shahfahad, N., & Rahman, A. (2025). Optimizing land use/land cover mapping accuracy: A comprehensive analysis of random forest with explainable artificial intelligence based feature importance analysis. *Journal of the Indian Society of Remote Sensing*, *53*(11), 3735–3754. https://doi.org/10.1007/s12524-025-02229-5

Rocha, B. M., Vieira, G. S., Fonseca, A. U., Sousa, N. M., Pedrini, H., & Soares, F. (2022). Detection of curved rows and gaps in aerial images of sugarcane field using image processing techniques. *Canadian Journal of Electrical and Computer Engineering*, *45*(3), 303–310. https://doi.org/10.1109/icjece.2022.3178749

Rouse, J. W., Haas, R. H., Schell, J. A., & Deering, D. W. (1974). Monitoring vegetation systems in the great plains with erts-1. *NASA Technical Reports Server (NASA)*, *1*, 309–317. http://hdl.handle.net/2060/19740022614

Rubini, P., & Kavitha, P. (2024). E2E model from crop suggestion to harvesting time prediction in sugarcane plant utilizing machine learning and deep learning. *Progress in Agricultural Engineering Sciences*, *20*(1), 233–270. https://doi.org/10.1556/446.2024.00139

Saad, S. A. K., & Al-Zubaidi, E. A. (2025). Classification of satellite Sentinel-2 imagery using unsupervised methods: A case study of Erbil. *AIP conference proceedings*, *3318*, 030028. https://doi.org/10.1063/5.0286607

Salberg, A.-B. (2011). Land Cover Classification of Cloud-Contaminated Multitemporal High-Resolution Images. *IEEE Transactions on Geoscience and Remote Sensing*, *49*(1), 377–387. https://doi.org/10.1109/tgrs.2010.2052464

Santos, E. R. D., Carvalho, W. D., & Mustin, K. (2025). Bibliometric analysis of global research on sugarcane production and its effects on biodiversity: trends, critical points, and knowledge gaps. *Conservation*, *5*(4), 67. https://doi.org/10.3390/conservation5040067

Shastry, A., Carter, E., Coltin, B., Sleeter, R., McMichael, S., & Eggleston, J. (2023). Mapping floods from remote sensing data and quantifying the effects of surface obstruction by clouds and vegetation. *Remote Sensing of Environment*, *291*, 113556. https://doi.org/10.1016/j.rse.2023.113556

Shendryk, Y., Rist, Y., Ticehurst, C., & Thorburn, P. (2019). Deep learning for multi-modal classification of cloud, shadow and land cover scenes in PlanetScope and Sentinel-2 imagery. *ISPRS Journal of Photogrammetry and Remote Sensing*, *157*, 124–136. https://doi.org/10.1016/j.isprsjprs.2019.08.018

Shi, D., & Yang, X. (2015, January 1). *Support vector machines for land cover mapping from remote sensor imagery*. https://doi.org/10.1007/978-94-017-9813-6_13

Soni, J., Prabakar, N., & Upadhyay, H. (2020, January). *Visualizing High-Dimensional Data using T-Distributed Stochastic neighbor Embedding Algorithm*. https://doi.org/10.1007/978-3-030-43981-1\{_}9

Subudhi, B. N., Bovolo, F., Ghosh, A., & Bruzzone, L. (2013). Spatio-contextual fuzzy clustering with Markov random field model for change detection in remotely sensed images. *Optics Laser Technology*, *57*, 284–292. https://doi.org/10.1016/j.optlastec.2013.10.003

Sujaritha, M., Annadurai, S., Satheeshkumar, J., Sharan, S. K., & Mahesh, L. (2017). Weed detecting robot in sugarcane fields using fuzzy real time classifier. *Computers and Electronics in Agriculture*, *134*, 160–171. https://doi.org/10.1016/j.compag.2017.01.008

Sujithra, J., & Ukrit, M. F. (2022). CRUN-Based leaf disease segmentation and Morphological-Based Stage Identification. *Mathematical Problems in Engineering*, *2022*, 1–13. https://doi.org/10.1155/2022/2546873

Tanut, B., & Riyamongkol, P. (2020). The Development of a Defect Detection Model from the High-Resolution Images of a Sugarcane Plantation Using an Unmanned Aerial Vehicle. *Information*, *11*(3), 136. https://doi.org/10.3390/info11030136

Thamoonlest, W., Posom, J., Saikaew, K., Phuphaphud, A., Chinapas, A., Panduangnat, L., & Saengprachatanarug, K. (2025). Forecasting gaps in sugarcane fields containing weeds using low-resolution UAV imagery based on a machine-learning approach. *Smart Agricultural Technology*, 100780. https://doi.org/10.1016/j.atech.2025.100780

Tucker, C. J. (1979). Red and photographic infrared linear combinations for monitoring vegetation. *Remote Sensing of Environment*, *8*(2), 127–150. https://doi.org/10.1016/0034-4257(79)90013-0

Tyukavina, A., Stehman, S., Foody, G., Bontemps, S., L., S., Olofsson, P., Tsendbazar, N., Radoux, J., Komarova, A., Serre, B., Song, X., d'Andrimont, R., Koren, G., Potapov, P., Bullock, E., Campbell, P., de Bruin, S., Defourny, P., Friedl, M., ... Xiao, X. (2025). Land cover and change map Accuracy Assessment and area Estimation Good Practices protocol. *IIASA PURE (International Institute of Applied Systems Analysis)*. https://doi.org/10.5067/doc/ceoswgcv/lpv/lc.001

Van Strien, M. J., & Grêt-Regamey, A. (2022). Unsupervised deep learning of landscape typologies from remote sensing images and other continuous spatial data. *Environmental Modelling Software*, *155*, 105462. https://doi.org/10.1016/j.envsoft.2022.105462

Vincini, M., & Frazzi, E. (2010). Comparing narrow and broad-band vegetation indices to estimate leaf chlorophyll content in planophile crop canopies. *Precision Agriculture*, *12*(3), 334–344. https://doi.org/10.1007/s11119-010-9204-3

Wagner, J., Nair, S. S., Skakun, S., Duncan, E. C., Li, F., Oliinyk, O., Nerry, F., Rehbinder, J., & Becker-Reshef, I. (2025). Monitoring cropland cultivation, abandonment, fallowing and recultivation dynamics with regard to conflict intensity in war-affected Ukraine. *Science of Remote Sensing*, *12*, 100326. https://doi.org/10.1016/j.srs.2025.100326

Wang, J., Yang, D., Chen, S., Zhu, X., Wu, S., Bogonovich, M., Guo, Z., Zhu, Z., & Wu, J. (2021). Automatic cloud and cloud shadow detection in tropical areas for planetscope satellite images. *Remote Sensing of Environment*, *264*, 112604. https://doi.org/10.1016/j.rse.2021.112604

Wang, M., Liu, Z., Baig, M. H. A., Wang, Y., Li, Y., & Chen, Y. (2019). Mapping sugarcane in complex landscapes by integrating multi-temporal Sentinel-2 images and machine learning algorithms. *Land Use Policy*, *88*, 104190. https://doi.org/10.1016/j.landusepol.2019.104190

Wang, Y., Belgiu, M., Wu, H., Zhong, D., Cao, Y., Li, H., & Tao, C. (2026). Joint learning for feature reconstruction and prediction in agricultural semantic segmentation from incomplete satellite image time series. *IEEE Transactions on Geoscience and Remote Sensing*, *64*, 1–23. https://doi.org/10.1109/TGRS.2025.3649017

Waters, E. K., Chen, C. C., & Azghadi, M. R. (2024). Sugarcane health monitoring with satellite spectroscopy and machine learning: A review. *Computers and Electronics in Agriculture*, *229*, 109686. https://doi.org/10.1016/j.compag.2024.109686

Williams, L., III, Halloran, S. T., Baker, P. D., Etzler, F. E., Lawrence, L. L., & Millar, J. G. (2025). Discovery and Field Evaluation of Sex Pheromone Components for the Click Beetle Melanotus verberans (LeConte) (Coleoptera: Elateridae). *Journal of Chemical Ecology*, *51*(1). https://doi.org/10.1007/s10886-025-01569-3

Wilson, S., Thorne, M. S., Wright, M. G., Peck, D. C., Mack, J., Fukumoto, G. K., & Curtiss, R. (2023). The twolined spittlebug (Hemiptera: Cercopidae) invades Hawaii: establishment, biology, and management of a destructive forage grass pest. *Journal of Integrated Pest Management*, *14*(1). https://doi.org/10.1093/jipm/pmad023

Wohlin, C. (2014, May). *Guidelines for snowballing in systematic literature studies and a replication in software engineering* (tech. rep.). https://doi.org/10.1145/2601248.2601268

Wright, M. N., & Ziegler, A. (2017). ranger: A fast implementation of random forests for high dimensional data in C++ and R. *Journal of Statistical Software*, *77*(1), 1–17. https://doi.org/10.18637/jss.v077.i01

Wright, N., Duncan, J. M., Callow, J. N., Thompson, S. E., & George, R. J. (2025). Training sensor-agnostic deep learning models for remote sensing: Achieving state-of-the-art cloud and cloud shadow identification with omnicloudmask. *Remote Sensing of Environment*, *322*, 114694. https://doi.org/10.1016/j.rse.2025.114694

Xu, H., Humpal, J. A., Wilson, B. A. L., Ash, G. J., & Powell, K. S. (2025). Yellow canopy syndrome of sugarcane: A review of current knowledge and future research directions. *Annals of Applied Biology*. https://doi.org/10.1111/aab.70040

Xu, J., Feng, G., Fan, B., Yan, W., Zhao, T., Sun, X., & Zhu, M. (2019). Landcover classification of satellite images based on an adaptive interval fuzzy c-means algorithm coupled with spatial information. *International Journal of Remote Sensing*, *41*(6), 2189–2208. https://doi.org/10.1080/01431161.2019.1685718

Xu, J., Zhao, T., Feng, G., Ni, M., & Ou, S. (2020). A fuzzy C-Means clustering algorithm based on spatial context model for image segmentation. *International Journal of Fuzzy Systems*, *23*(3), 816–832. https://doi.org/10.1007/s40815-020-01015-4

Yadav, R., Singh, D., & Bhatnagar, A. (2013). Growth, sugar yield and profitability of spring sugarcane as influenced by sett size, seed rate and sett treatment. *Madras Agricultural Journal*, *100*(july), 726–729. https://doi.org/10.29321/maj.10.001392

Yahaya, A., Dangora, D. B., Kumar, P. L., Alegbejo, M. D., Gregg, L., & Alabi, O. J. (2018). Prevalence and genome characterization of field isolates of sugarcane mosaic virus (SCMV) in Nigeria. *Plant Disease*, *103*(5), 818–824. https://doi.org/10.1094/pdis-08-18-1445-re

Yaras, C., Kassaw, K., Huang, B., Bradbury, K., & Malof, J. M. (2023). Randomized histogram matching: a simple augmentation for unsupervised domain adaptation in overhead imagery. *IEEE Journal of Selected Topics in Applied Earth Observations and Remote Sensing*, *17*, 1988–1998. https://doi.org/10.1109/jstars.2023.3340412

Ying, Y., Cui, X., Li, H., Pan, L., Luo, T., Cao, Z., & Wang, J. (2023). Development of magnetic lateral flow and direct competitive immunoassays for sensitive and specific detection of Halosulfuron-Methyl using a novel hapten and monoclonal antibody. *Foods*, *12*(14), 2764. https://doi.org/10.3390/foods12142764

Zarcotejada, P., Berjon, A., Lopezlozano, R., Miller, J., Martin, P., Cachorro, V., Gonzalez, M., & Defrutos, A. (2005). Assessing vineyard condition with hyperspectral indices: Leaf and canopy reflectance simulation in a row-structured discontinuous canopy. *Remote Sensing of Environment*, *99*(3), 271–287. https://doi.org/10.1016/j.rse.2005.09.002

Zhou, D., Wang, C., Li, Z., Chen, Y., Gao, S., Guo, J., Lu, W., Su, Y., Xu, L., & Que, Y. (2016). Detection of Bar Transgenic Sugarcane with a Rapid and Visual Loop-Mediated Isothermal Amplification Assay. *Frontiers in Plant Science*, *7*. https://doi.org/10.3389/fpls.2016.00279

Generative AI statement

Generative AI was utilised during the writing of this internship report for spelling and grammar checking, as well as improving the scientific writing where necessary. Generative AI was further used as help tool during scripting and LaTeX formatting. The Claude Sonnet 4.5 model with reasoning was used through Perplexity. The model was set to ground using scientific articles and web searches. All prompts and answers have been made available in a Perplexity space, available here.

Appendixes

Appendix I

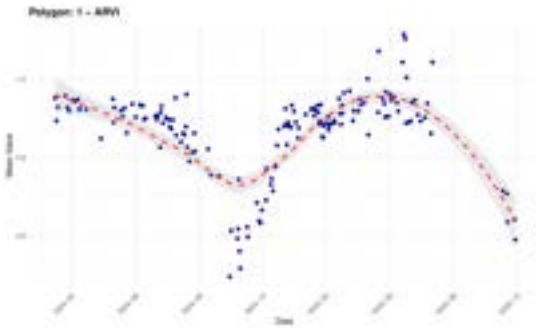

(a) Long-term trend for average ARVI value

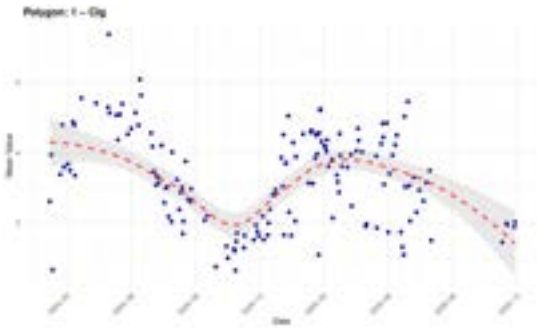

(b) Long-term trend for average CIg value

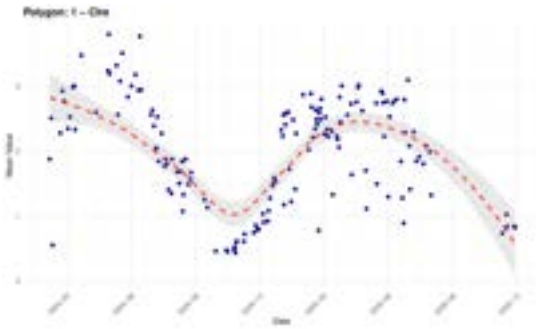

(c) Long-term trend for average CIre value

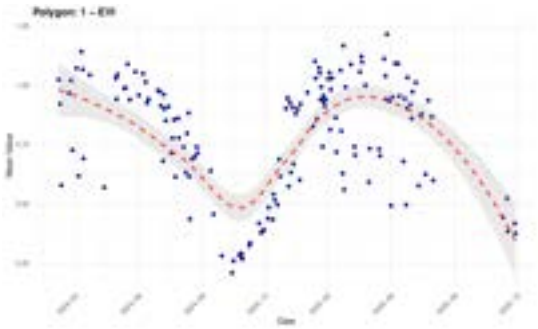

(d) Long-term trend for average EVI value

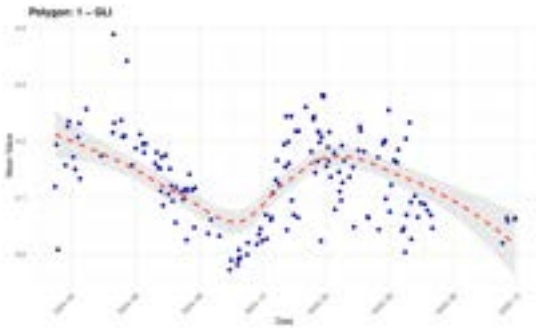

(e) Long-term trend for average GLI value

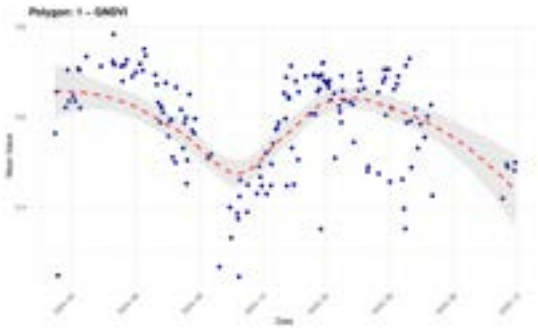

(f) Long-term trend for average GNDVI value

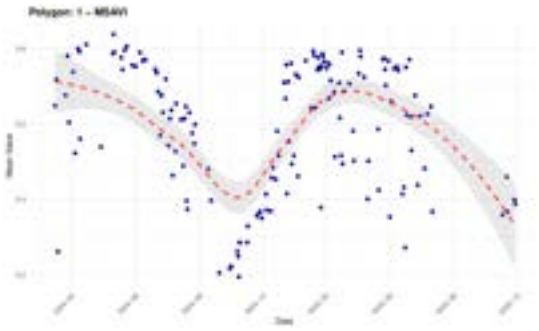

(g) Long-term trend for average MSAVI value

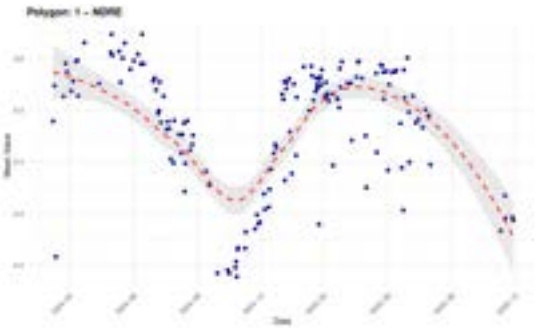

(h) Long-term trend for average NDRE value

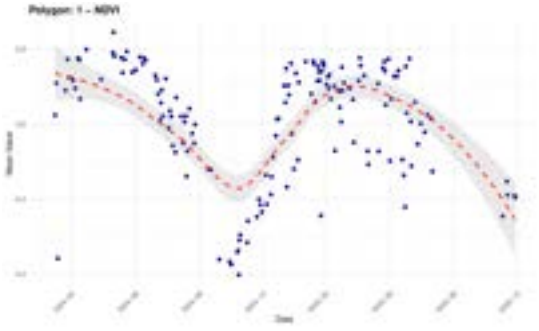

(i) Long-term trend for average NDVI value

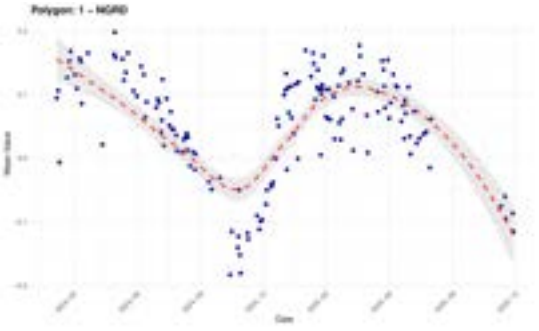

(j) Long-term trend for average NGRD value

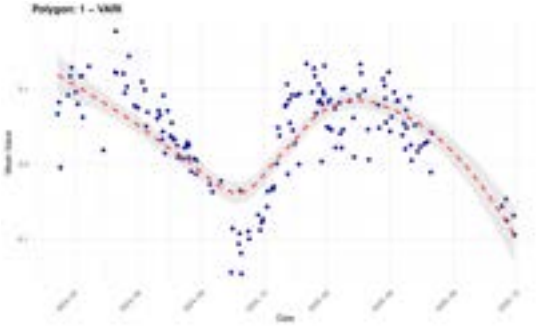

(k) Long-term trend for average VARI value

Long-term trends for spectral indices

Appendix II

Ten variables with highest variable importance for supervised classifiers based on spatial hold-out testing

Note: Importances for LSVM, RSVM and LDA are averaged across the classes, as these provide class-specific levels of importance.

Importance	**RF Model**	**XGB**	**LSVM**	**RSVM**	**LDA**
1	MSAVI (0.12)	MSAVI (0.34)	NDVI (0.99)	NDVI (0.99)	NDRE (0.98)
2	EVI (0.10)	NDVI (0.19)	ARVI (0.98)	ARVI (0.98)	CVI (0.59)
3	NDVI (0.09)	BGI (0.12)	NGRD (0.98)	NGRD (0.98)	BGI (0.97)
4	NGRD (0.07)	GLI (0.10)	VARI (0.98)	VARI (0.98)	ΔARVI (0.77)
5	ARVI (0.07)	ΔARVI (0.07)	GNDVI (0.98)	GNDVI (0.97)	ΔVARI (0.64)
6	VARI (0.07)	ARVI (0.07)	NDRE (0.98)	NDRE (0.98)	ΔEVI (0.68)
7	GLI (0.06)	GNDVI (0.03)	EVI (0.98)	EVI (0.99)	ΔCVI (0.74)
8	NDRE (0.03)	VARI (0.02)	CVI (0.58)	CVI (0.59)	ΔBGI (0.70)
9	BGI (0.03)	ΔCIg (0.01)	BGI (0.97)	BGI (0.97)	ΔGLI (0.71)
10	CIre (0.03)	EVI (0.01)	GLI (0.99)	GLI (0.99)	–

Appendix III

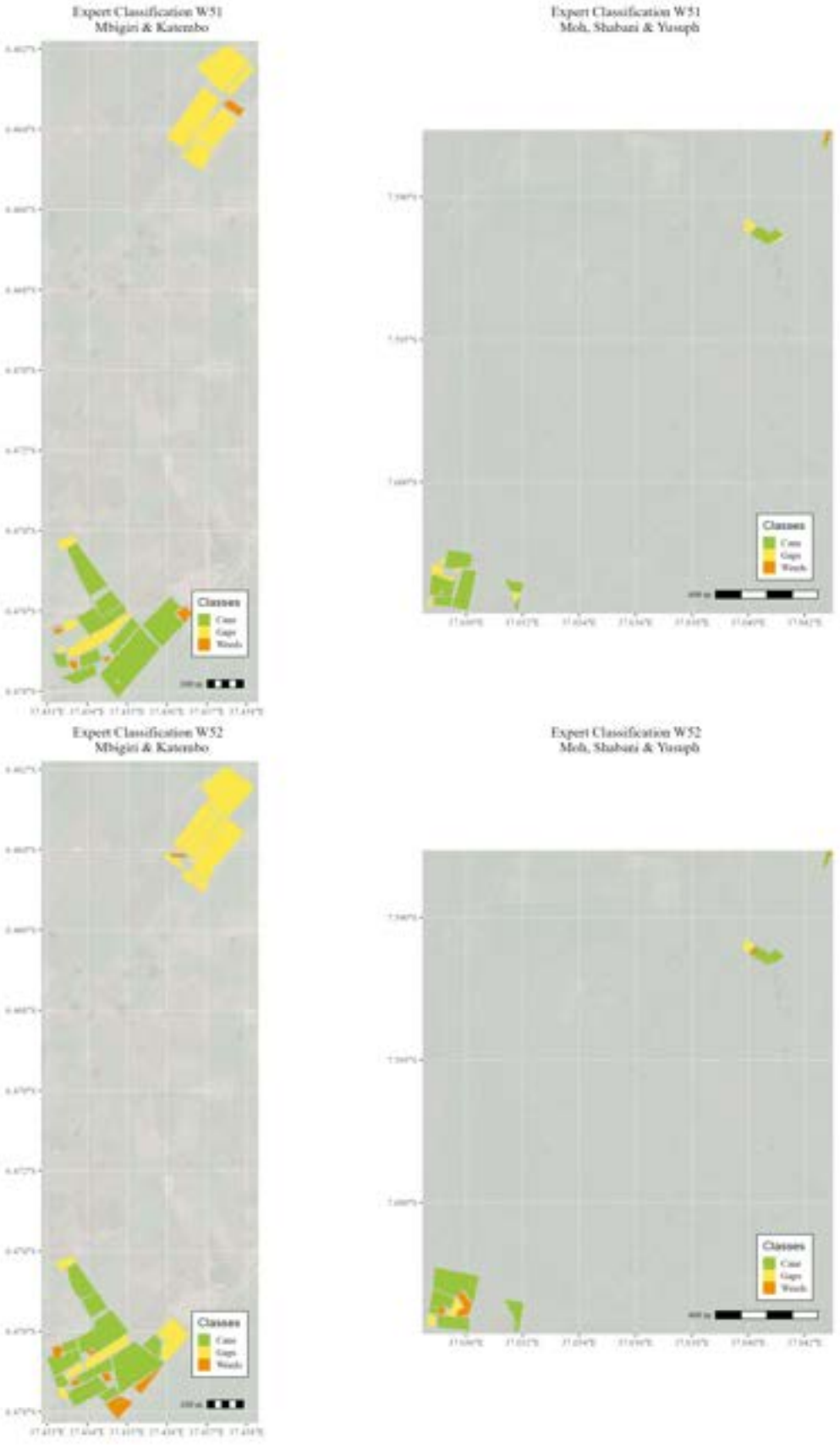

Overview of expert validation classes for weeks 51 and 52.

Appendix IV

Overview of supervised consensus classification for weeks 51 and 52.

Appendix V

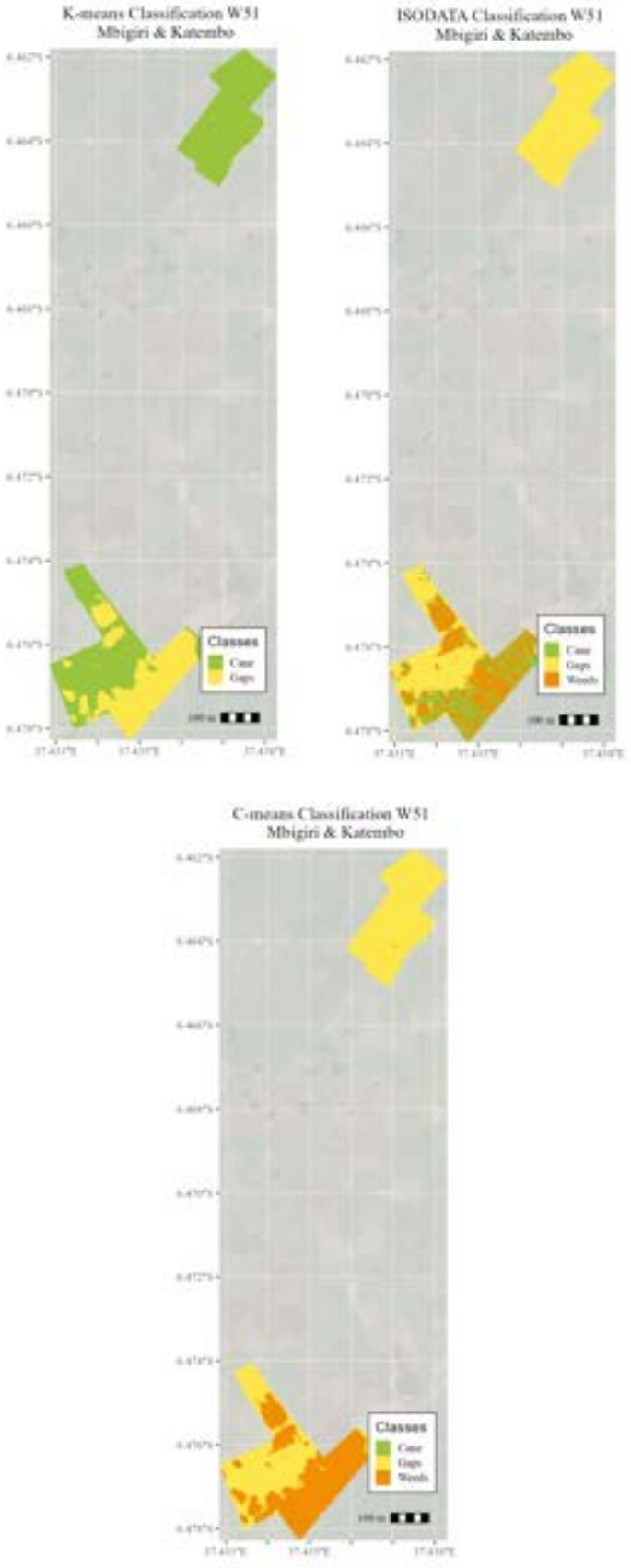

Overview of unsupervised classifications for fields Mbigiri and Katembo in week 51.